Published online 28 June 2017

Nucleic Acids Research, 2017, Vol. 45, No. 15 ***9121–9137***
doi: 10.1093/nar/gkx559

Human ribosomal protein eS1 is engaged in cellular events related to processing and functioning of U11 snRNA

Alexander V. Gopanenko[1,2], Alexey A. Malygin[1,2], Alexey E. Tupikin[1], Pavel P. Laktionov[1], Marsel R. Kabilov[1] and Galina G. Karpova[1,2,*]

[1]Institute of Chemical Biology and Fundamental Medicine, Siberian Branch of the Russian Academy of Sciences, Novosibirsk 630090, Russia and [2]Department of Molecular Biology, Novosibirsk State University, Novosibirsk 630090, Russia

Received September 20, 2016; Revised June 15, 2017; Editorial Decision June 16, 2017; Accepted June 20, 2017

ABSTRACT

Ribosomal proteins are involved in many cellular processes through interactions with various RNAs. Here, applying the photoactivatable-ribonucleoside-enhanced cross-linking and immunoprecipitation approach to HEK293 cells overproducing ribosomal protein (rp) eS1, we determined the products of *RNU5A-1* and *RNU11* genes encoding U5 and U11 snRNAs as the RNA partners of ribosome-unbound rp eS1. U11 pre-snRNA-associated rp eS1 was revealed in the cytoplasm and nucleus where rp eS1-bound U11/U12 di-snRNP was also found. Utilizing recombinant rp eS1 and 4-thiouridine-containing U11 snRNA transcript, we identified an N-terminal peptide contacting the U-rich sequence in the Sm site-containing RNA region. We also showed that the rp eS1 binding site on U11 snRNA is located in the cleft between stem-loops I and III and that its structure mimics the respective site on the 18S rRNA. It was found that cell depletion of rp eS1 leads to a decrease in the splicing efficiency of minor introns and to an increase in the level of U11 pre-snRNA with the unprocessed 3′ terminus. Our findings demonstrate the engagement of human rp eS1 in events related to the U11 snRNA processing and to minor-class splicing. Contacts of rp eS1 with U5 snRNA in the minor pre-catalytic spliceosome are discussed.

INTRODUCTION

Eukaryotic ribosomal proteins, being indispensable constituents of the cellular translation machine—ribosome, are involved in the maintenance of the architecture and functioning of its two subunits, the small (40S) and large (60S) ones (1). Human ribosome consists of 80 different proteins bound predominantly to four structured rRNAs that serve as a scaffold for the overall ribosome construction (2,3). Being synthetized in the cytoplasm, most of ribosomal proteins are then imported into the cell nucleus and further into the nucleolus, the place of assembly of the ribosomal subunits (4,5), and on this way, they can be recruited as RNA-binding proteins in some specific processes occurring beyond the ribosome.

To date, there are numerous reports indicating that individual ribosomal proteins act as participants in splicing (uS15 (6), eS26 (7) and uL3 (8)), DNA repair (uS3 (reviewed in (9))), mRNA-specific translation control (uL13 (10)), cell signaling (RACK1 (11)) and in several other processes (for a review, see (12)). The diversity of the discovered extra-ribosomal functions of ribosomal proteins implies that the actual list of proteins having such functions might be much longer. Therefore, the systematic investigations on the search for cellular RNA partners of the particular human ribosomal proteins could reveal molecular interaction networks that involve these proteins as key players in the events providing different stages of cellular life.

Human ribosomal protein (rp) eS1 (previously classified as S3A) lacking eubacterial counterparts is actively engaged in the functioning of translation machinery as the 40S ribosomal subunit component participating in the binding of translation factor eIF3 (13) as well as in the organization of binding site for the Internal Ribosome Entry Site (IRES) element of hepatitis C virus (14–17). However, very little is known about the processes, in which rp eS1 is implicated as a player being outside the ribosome. For example, the ability to interact with rp eS1 has been described for poly (ADP-ribose) polymerase (PARP) (18) and transcription factor CCAAT-enhancer-binding protein homologous protein (CHOP) (19). Particularly, the binding of rp eS1 to PARP assisted apoptosis regulator Bcl-2 in the inhibition of PARP activity, leading to the prevention of apoptosis (18), whereas the interaction of rp eS1 with CHOP blocked the

*To whom correspondence should be addressed. Tel: +7 383 363 5140; Fax: +7 383 363 5153; Email: karpova@niboch.nsc.ru

activity of CHOP as a factor responsible for the erythroid differentiation of cells and thereby inhibited the differentiation induced by erythropoietin (19). No specific contacts between rp eS1 and cellular RNAs other than rRNA have yet been reported, although the protein is positively charged and could readily interact with RNA.

In this work, using photoactivatable-ribonucleoside-enhanced cross-linking and immunoprecipitation (PAR-CLIP) approach, we performed a search for RNAs, which could be the binding partners of rp eS1 in human cells. A potential rp eS1 site, which would provide the protein interaction with these RNAs, was predicted to be located at the very end of the N-terminal portion of rp eS1. To apply PAR-CLIP approach to human cells, we obtained HEK293 cell line inducibly generating FLAG-tagged rp eS1 (^{FLAG}eS1) and showed that the ectopically produced target protein was able to substitute native rp eS1 in the translating ribosome. The cells treated with 4-thiouridine were revealed to produce RNA-^{FLAG}eS1 cross-links much effectively than those treated with 6-thioguanosine. Next generation sequencing (NGS) of RNA fragments cross-linked to the target protein revealed products of *RNU5A-1* and *RNU11* genes encoding U5 and U11 snRNAs as the main partners of rp eS1, besides rRNA. The respective cross-linking sites were established by identifying the characteristic T/C transitions in the NGS data. The mapping of these sites onto the snRNA structures allowed the determination of U-rich sequences corresponding to an Sm site-containing single-stranded region in U11 snRNA and to stem-loop (SL) I in U5 snRNA as structural elements of RNAs transcribed from the above genes that take part in the binding to rp eS1. Immunoprecipitation of nuclear and cytoplasmic extracts of HEK293 cells with anti-rp eS1 antibodies followed by reverse transcriptase polymerase chain reaction (RT-PCR) analysis revealed rp eS1-associated U11 pre-snRNA both in the nucleus and in the cytoplasm and, in addition, U11/U12 di-snRNP in the nucleus, whereas rp eS1-bound U5 pre-snRNA/U5 snRNA was not detected. *In vitro* binding assays utilizing recombinant $(His)_6$-tagged ^{FLAG}eS1 (^{His6}eS1) and T7 transcripts corresponding to U11 snRNA and its truncated form lacking a 3′-terminal fragment containing the Sm site (U11 snRNA(ΔSm)), together with studying the inhibitory effect of octauridylate, $(pU)_8$, on the binding of the protein to U11 snRNA, showed a significant contribution of the Sm-comprising U-rich sequence of U11 snRNA to this binding. It turned out that ribosome-bound rp eS1 was unable to bind to the U11 snRNA at all. Chemical footprinting of U11 snRNA bound to ^{His6}eS1 displayed the multiple protections of nucleotides in the regions of SLI, SLIII, H-helix and Sm site from attack by various probes as well as the enhanced reactivity to benzoyl cyanide (BzCN) of the RNA backbone in the U-rich single-stranded sequence. A comparison of the spatial structures of the U1 snRNA region homologous to that containing the rp eS1 binding site in U11 snRNA and of the 40S ribosomal subunit area comprising the rp eS1-bound fragment of the 18S rRNA revealed their similarity. With ^{His6}eS1 cross-linked to 4-thiouridine-containing U11 snRNA, we identified a short peptide 9–29 within the N-terminal region of rp eS1 that is involved in the cross-linking. HEK293 cells depleted of rp eS1 were shown to exhibit an increased level of U11 pre-snRNA with the unprocessed 3′ end and a decrease in splicing efficiency of the minor class introns. Our findings provide for the first time the evidence for the engagement of the ribosome-unbound rp eS1 in cellular events related to the processing and functioning of U11 snRNP and suggest that rp eS1, when bound to U11 snRNA, may also interact with U5 snRNA in the minor pre-catalytic spliceosome.

MATERIALS AND METHODS

Plasmids preparation, cells transfection, stable cell line generation and immunoblotting

The pCI-neo vector (Promega) was used in the preparation of the plasmid for DOX-inducible expression system of the target gene. The sequence of rtTA (reverse tetracycline trans-activator) gene was amplified using the FUdeltaGW-rtTA vector (Addgene) as a template and a pair of primers 1F and 1R (here and further the primer sequences are given in Supplementary Table S1), and inserted into pCI-neo at the restriction sites SalI and XhoI, resulting in plasmid pCI-neo-rtTA. The TRE-CMV_{min} sequence was amplified using vector TetO-FUW-OSKM (Addgene) and a pair of primers 2F and 2R. PolyA signal sequence was amplified using the pCI-neo and primers 4F and 4R. The multiple cloning site (MCS) was generated using the complementary oligodeoxiribonucleotides 3F and 3R. Construction containing the sequences of TRE_CMV_{min}, MCS and polyA signal was obtained by overlapping PCR using the respective amplified products and primers 2F and 4R. Resulting PCR product was digested with BamHI and inserted into the pCI-neo-rtTA at BglII site, given plasmid pAG-1. The minigene FLAG-eS1 amplified with the use of HEK293 cDNA and primers 5F and 5R was inserted into pAG-1 at EcoRI site by blunt ligation in forward direction. The resulting plasmid was linearized by BamHI with its subsequent utilization for the HEK293 cells (ATCC CRL-1573) transfection performed with the use of Lipofectamin LTX (Invitrogen). For stable production of the target protein, the transfected cells were selected with G-418. Stable clones were tested for their ability to produce ^{FLAG}eS1 after doxycycline (DOX) induction by either western blotting with the use of anti-FLAG M5 (Sigma, #F4042) or immunoprecipitation with the use of anti-FLAG M2 (Sigma, #F1804) with subsequent western blotting utilizing specific goat polyclonal antiserum against rat rp eS1 (anti-rp eS1) (kindly gifted by Dr J. Stahl). In the western blotting, the protein G-HRP-conjugate and Western Blotting Substrate kit (Thermo Fisher Scientific) were applied to reveal primary antibodies bound on a membrane and the membrane was exposed at ChemiDoc XRS system (BioRad).

Analysis of ^{FLAG}eS1 incorporation into ribosomes

The polysome profiles were obtained as described (20) with some modifications. Stable HEK293 cells producing ^{FLAG}eS1 were used for polyribosomes isolation by the following procedure. Cells were cultured in 15 cm Petri dish containing Dulbecco's modified Eagle's medium (DMEM), 10% FBS and penicillin–streptomycin 100 U/ml (all from Thermo Fisher Scientific) at CO_2-incubator (5% CO_2) at

37°C. At 40–50% confluency, DOX was added to 2 μg/ml. After 48 h, cycloheximide was added to concentration of 100 μg/ml and cells were incubated for 15 min at 37°C, and then washed with ice-cold phosphate buffered saline (PBS). Then, cells were collected by brief centrifugation at 1000 *g* at 4°C and lysed in 20 mM HEPES-KOH buffer (pH 7.5) containing 15 mM $MgCl_2$, 200 mM KCl, 1% Triton-X100, 2 mM dithiothreitol (DTT), 100 μg/ml cycloheximide and 0.025 U/μl RiboLock RNase Inhibitor (Thermo Fisher Scientific). Lysate was clarified by centrifugation at 14 000 rpm for 10 min at 4°C, layered onto a 7 to 47% linear sucrose gradient in 50 mM Tris–HCl buffer (pH 7.5) containing 50 mM NH_4Cl, 12 mM $MgCl_2$ and 1 mM DTT and centrifuged at 100 000 *g* for 4.5 h at 4°C. Gradients were fractioned with monitoring of the UV absorption profiles at A_{260}. Total protein in fractions was isolated using Strata-Clean beads (Stratagene) and analyzed by western blotting using anti-FLAG M5. Experiment was replicated in triplicate.

PAR-CLIP analysis of the transfected HEK293 cells ectopically producing ^{FLAG}eS1

The experiments were carried out as described (21) with some modifications. Typically, 10 of 15 cm dishes of adherent HEK293 cells DOX-inducibly producing N-terminal ^{FLAG}eS1 were cultured as above. At 70–80% confluency, culture medium was freshly changed; DOX (2 μg/ml) and photoactivatable 4-thiouridine or 6-thioguanosine (250 μM) were then added to the cells. After 48 h, culture medium was removed and cells were washed with PBS. Cross-linking was performed by irradiation of cells with UV light at 312 nm (0.15–0.5 J/cm^2) in Bio-Link (Vilber Lourmat) on ice; cells were washed with ice-cold PBS and collected by centrifugation at 1000 *g*.

The cell pellet was lysed in three volumes of 25 mM Tris–HCl buffer (pH 7.5) containing 150 mM NaCl, 1% NP-40, 0.5 mM DTT, 5% glycerol, 1 mM ethylenediaminetetraacetic acid (EDTA), protease inhibitor cocktail (Sigma) and 20 U/ml DNase I. The lysate was incubated on ice for 10 min, triturated through 29 G needle 10 times, clarified by centrifugation at 20 000 *g* for 10 min at 4°C and passed through the 0.22 μm syringe-filter (TPP). The supernatant was then transferred to a new non-stick tube. RNase T1 was added to the supernatant to 1 U/μl and the reaction mixture was incubated at room temperature for 15 min. The mixture was clarified by centrifugation as above and anti-FLAG M2 antibodies-bound magnetic Protein G beads (Dynabeads, Life Technologies) were added to the supernatant. In typical experiment, 10 μg of the antibodies were bound to 40 μl of Protein G Dynabeads in PBS containing 0.05% Tween-20 for 1 h at 4°C. Immunoprecipitation was carried out on a rotating platform for 1 h at 4°C. After the supernatant removing, the beads were washed three times with 1 ml of buffer 50 mM Tris–HCl (pH 7.5) containing 300 mM KCl, 0.05% NP-40 and 0.5 mM DTT and resuspended in one volume of the same buffer. RNase T1 was added to the bead's suspension to 20 U/μl and the mixture was incubated for 20 min at ambient temperature on a rotating platform as above. The beads were washed three times with 1 ml of the buffer containing 50 mM Tris–HCl (pH 7.5), 500 mM KCl, 0.05% NP-40 and 0.5 mM DTT and twice in 1 ml of the Dephos buffer containing 50 mM Tris–HCl (pH 7.5), 100 mM NaCl, 10 mM $MgCl_2$ and 1 mM DTT and then resuspended in one volume of the Dephos buffer**.** Calf intestinal phosphatase (NEB) was added to the bead's suspension to 0.5 U/μl, the mixture was incubated on shaker for 10 min at 37°C and the supernatant was removed. The beads were washed twice in 1 ml of Phos-wash buffer containing 50 mM Tris–HCl (pH 7.5), 20 mM and 0.5% NP-40 and twice in 1 ml of T4 polynucleotide kinase (PNK) buffer containing 50 mM Tris–HCl (pH 7.5), 50 mM NaCl, 10 mM $MgCl_2$ and no DDT. After washing, the beads were resuspended in 50 μl of PNK reaction mixture containing 50 mM Tris–HCl (pH 7.5), 50 mM NaCl, 10 mM $MgCl_2$, 5 mM DTT, 0.5 μCi/μl of γ-^{32}P-ATP (adenosine triphosphate) and 1 U/μl of T4 PNK (NEB) with subsequent incubation of the bead's suspension on a shaker for 30 min at 37°C. ATP was then added to the suspension to a concentration of 1 mM and the mixture was incubated for 5 min at 37°C. Finally, the beads were washed five times with 1 ml of PNK buffer and resuspended in 50 μl of sodium dodecyl sulfate polyacrylamide gel electrophoresis (SDS-PAGE) loading buffer containing 10% glycerol, 50 mM Tris–HCl (pH 6.8), 2 mM EDTA, 2% SDS, 100 mM DTT and 0.1% bromophenol blue.

The beads suspension was incubated on a shaker for 5 min at 95°C, beads were separated by a magnetic separator, the supernatant was transferred to a non-stick tube and the remaining beads were removed by brief centrifugation. The supernatant was subjected to 15% SDS-PAGE and protein–RNA cross-links were transferred onto nitrocellulose membrane with subsequent autoradiography onto a Kodak phosphorimager screen and analysis in FX Pro Plus MultiImager (Bio-Rad). The location of rp eS1 on the membrane was determined by western blotting of the aliquoted samples with anti-rp eS1 antiserum.

To isolate cross-linked RNA, membrane slices containing ^{32}P-label were incubated with 100 μl of mixture containing Proteinase K buffer (50 mM Tris–HCl (pH 7.5), 75 mM NaCl, 6 mM EDTA and 1% SDS) and 1 mg/ml of Proteinase K on a thermoshaker for 30 min at 37°C. After the incubation, 400 μl of Proteinase K buffer was added to the membrane slices and RNA was eluted for 4 h at room temperature. After phenol–chloroform deproteination of the eluate, it was supplemented with 2 μl of GlycoBlue and NaOAc (pH 5.0) to 0.3 M and RNA was precipitated by 500 μl of isopropanol followed by overnight incubation at −80°C and centrifugation at 20 000 *g* for 30 min at 4°C. The RNA pellet was resuspended in 10 μl of nuclease-free water.

PAR-CLIP libraries preparation and bioinformatics analysis of sequencing data

PAR-CLIP libraries were prepared using NEBNext Small RNA Library Prep Set for Illumina (NEB) according to the manufacturer's protocols. For size selection, the libraries were loaded on 2% Agarose Dye Free Gel Cassettes (Sage Science) and fragments of 125–180 bp were isolated with Blue Pippin DNA size selection system (Sage Science) according to the manufacturer's instructions.

The sequencing of the libraries was performed on MiSeq (Illumina) genomic sequencer with the Reagent Kit v3 (150 cycles, Illumina). The read data reported in this study were submitted to the GenBank under the study accession PRJNA337889 and the sample accession SRP080974. These data are the results of PAR-CLIP experiments carried out with and without transferring of cross-links onto a membrane as well as of controls to them performed without UV-irradiation.

Fastq reads were analyzed using tools of the CLC GW 9.0 software (Qiagen). Reads were filtered for both the quality (ambiguous limit, 2; quality limit, 0.031) and adapter sequences, and then mapped to the sequences corresponding to 45S (NR_046235) and 5S (NR_023363) rRNAs using the Mapped reads to reference tool (length fraction, 0.8; similarity fraction, 0.8; other parameters by default). Unmapped reads were mapped to human reference genome (hg38) with Ensemble annotation GRCh38.88 by the RNA-Seq analysis tool (length fraction, 0.8; similarity fraction, 0.8; strand specific, forward, and other parameters by default). PAR-CLIP peaks were detected using the transcription factor ChIP-Seq analysis tool with default settings (maximal *P*-value, 0.1). T/C transitions were found by the basic variant detection tool with parameters (ploidy, 2; ignore broken reads, no; ignore non-specific matches, no; minimum coverage, 10; minimum count, 2; frequency, 1–95%; relative read direction filter, no; other parameters by default) and those, which were also found in the controls to PAR-CLIP experiments, were excluded from further consideration.

Immunoprecipitation of the rp eS1-containing RNPs from nuclear and cytoplasmic fractions of HEK293 cells and analysis of the RNA content therein

Typically, 10^8 pelleted HEK293 cells were resuspended in 3 ml of the buffer containing 25 mM Tris–HCl (pH 7.5), 150 mM NaCl, 1mM EDTA, 0.5% NP-40 and 30 μl of protease inhibitor cocktail (Sigma), and nuclei were pelleted by centrifugation at 1800 *g* for 1 min at 4°C. The resulting supernatant was then clarified by centrifugation at 20 000 *g* for 10 min at 4°C to obtain the cytoplasmic fraction. The nuclei pellet was resuspended in 3 ml of the same buffer that contained 1% NP-40 and additionally 5% glycerol The suspension was passed through a 29 G syringe needle for 10 times and clarified by centrifugation at 20 000 *g* for 10 min at 4°C to obtain the nuclear fraction in the supernatant. One milliliter of the cytoplasmic or nuclear fractions was supplemented with 30 μl of Dynabeads coupled with anti-rp eS1 antibodies with subsequent incubation for 1 h at 4°C to immunoprecipitate the rp eS1-containing RNPs. Beads were then washed three times with 1 ml of the buffer containing 20 mM Tris–HCl (pH 7.5), 300 mM KCl and 0.5% NP40. To elute RNA, 50 μl of 20 mM Tris–HCl (pH 7.5) containing 1% SDS were added to the beads and after heating at 95°C for 5 min, RNA was recovered by phenol–chloroform deproteination and ethanol precipitated. cDNA from RNA isolated from the cytoplasmic or nuclear fractions was prepared utilizing random $d(N)_6$ primer and SuperScript IV reverse transcriptase (Thermo Fisher Scientific) according to the manufacturer's protocol, and PCR reactions were performed in total volume of 20 μl using 0.1 ng of the cDNA. Pairs of primers RNU11_Frt and preRNU11_Rrt, RNU11_Frt and 11R, and 12F and 12R were utilized to amplify the fragments of the U11 pre-snRNA, U11 snRNA and U12 snRNA, respectively, from the cytoplasmic and nuclear cDNAs, and primers 9F and 9R were used to amplify the fragment of U5 snRNA from nuclear cDNA. The resulting PCR products were resolved on a 3% agarose gel, stained with ethidium bromide and detected using Chemi-Doc XRS (BioRad).

Recombinant ^{His6}eS1 preparation

The rp eS1 coding sequence was obtained by PCR amplification using primers 6F and 6R and cloned into pET15b at NdeI and BamHI sites, so that the encoded protein contained both $(His)_6$ and FLAG tags at the N-terminus. *Escherichia coli* BL21(DE3) cells transformed by the resulting plasmid were grown at 37°C; protein production was then induced by adding of isopropyl β-D-1-thiogalactopyranoside (IPTG) to 1 mM and the culture was incubated further for 6 h at 18°C. ^{His6}eS1 was purified on Ni-NTA resin, dialyzed against 20 mM HEPES-KOH buffer (pH 7.5) containing 100 mM KCl, 0.05% Tween-20 and 1 mM β-mercaptoethanol and concentrated; glycerol was added to 50% before storage.

Synthesis of snRNAs by *in vitro* T7 transcription

DNA templates for the synthesis of U11 and U5 snRNAs were obtained by PCR amplification of HEK293 genomic DNA with the use of forward and reverse primers specific for sequences of *RNU11* (11F and 11R) and *RNU5A-1* (9F and 9R) genes. The resulting products were cloned in pUC19 at SmaI site. The DNA templates also contained T7 promoter and the sequence corresponding to the T3 sequencing primer. ^{32}P-labeled RNA transcripts were prepared by T7 transcription using the respective DNA templates as described in (22), purified in denaturing PAGE, eluted and ethanol precipitated. Randomly 4-thiouridine-containing RNAs were obtained as above with the application of UTP to 4-thio-UTP analog ratio as 5 to 1.

Analysis of the ^{His6}eS1 *in vitro* binding to the snRNA transcripts

To test the binding, both nitrocellulose filter binding and gel electrophoresis mobility shift assays called as NCFBA and EMSA, respectively, were applied. Binding of ^{His6}eS1 to the snRNA transcripts was carried out in 20 μl of the binding buffer containing 20 mM HEPES-KOH (pH 7.5), 100 mM KCl and 2.5 mM $MgCl_2$ (buffer B) and supplemented with 0.05% Triton X-100 and 1 mM β-mercaproethanol for 30 min at 25°C. The protein concentration in the mixtures varied from 0.1 nM to 1 mM; the RNA concentration was <0.1 nM. When the NCFBA was used, filters with pores of 0.45 μm (GE Healthcare) were utilized and the radioactivity retained on the filters was counted as described (23). In the EMSA-experiments, glycerol was added to the mixtures up to a final concentration of 5% prior their loading onto gel. Free and protein-bound RNAs were separated under native

conditions in 6% PAGE in Tris-glycine buffer (25 mM Tris and 200 mM glycine) on ice. After the electrophoresis, gel was dried and autoradiographed as above. All EMSA and NCFBA experiments were reproduced in triplicate.

Chemical footprinting of U11 snRNA transcript bound to ^{His6}eS1

Binding of U11 snRNA transcript to ^{His6}eS1 was carried out in buffer B supplemented with 5% glycerol as described above using 1 μM U11 snRNA and 2 μM ^{His6}eS1. Probing of RNA with 1-cyclohexyl-(2-morpholinoethyl)carbodiimide metho-p-toluene sulfonate (CMCT) was performed by addition of one third volume of freshly made 200 mM CMCT in 50 mM HEPES-KOH (pH 8.0) to the prepared mixture. After 15 min incubation at 37°C, the reaction was stopped by adding β-mercaptoethanol to final concentration of 100 mM and the RNA was isolated by phenol deproteination and ethanol precipitation. Probing of RNA with BzCN was carried out by treatment of the mixture with 80 mM BzCN for 2 min at room temperature. The reaction was stopped by adding one volume of water and RNA was immediately isolated as above. Probing of RNA with hydroxyl radicals was performed as described (16).

For reverse transcription, reaction mixtures of 10 μl containing 1–2 pmol of RNA, 5 pmol of 5′-^{32}P labeled T3-primer, 0.5 mM dNTPs and 1 unit of AMV reverse transcriptase (Invitrogene) in 50 mM Tris–HCl (pH 8.3) buffer containing 75 mM KOAc, 8 mM $Mg(OAc)_2$ and 10 mM DTT were incubated for 30 min at 42°C. The reaction products were ethanol precipitated, dissolved in formamide containing 0.1% bromophenol blue and 0.1% xylene cyanol, and separated in denaturing 8% PAGE. The dried gel was autoradiographed as above. All the experiments were reproduced at least in triplicate.

Cross-linking of 4-thiouridine-containing U11 snRNA to ^{His6}eS1 and identification of the cross-linking sites in the protein and the RNA

Binding of the randomly containing 4-thiouridine ^{32}P-labeled U11 snRNA transcript to ^{His6}eS1 was carried out as described above for the unmodified RNA. Reaction mixture was UV-irradiated at 312 nm (0.15–0.5 J/cm^2) on ice in Bio-Link. The mixture was treated with RNase T1 (50 U/μl) for 10 min at 37°C and the RNA–protein cross-links were separated in 15% SDS-PAGE. The gel piece corresponding to the RNA–protein cross-links was excised, vacuum dried and applied in cleavage by iodosobenzoic acid (IOBz), cyanogen bromide (CNBr) or endopeptidase ArgC. With CNBr cleavage, the gel piece was incubated in 100 μl of 70% formic acid containing 0.25 M CNBr overnight at room temperature and solution of the eluted peptides was vacuum dried. With IOBz cleavage, the gel piece was incubated with 100 μl of solution containing 60 mg/ml IOBz, 80% acetic acid and 1.5 M guanidine-HCl overnight at 37°C and peptides were precipitated by 1 ml of EtOH with subsequent centrifugation at 20 000 *g* for 30 min at 4°C. With ArgC cleavage, the gel piece was treated with 100 μl of solution containing 25 mM Tris–HCl (pH 7.5), 5 mM $CaCl_2$, 2 mM EDTA, 5 mM DTT and 0.01 μg/μl Arg-C and incubated overnight at 37°C; the solution of eluted peptides was vacuum dried. The resulting peptides were resolved in 16.5% tris-tricine SDS-PAGE. Ultra-low molecular weight marker (MW 1.1–26.6 kDa, Sigma) was used as a marker. Gel was dried and autoradiographed as above. To carry out additional cleavages, the ^{His6}eS1 peptides obtained by the digestion with CNBr or ArgC and resolved in tris-tricine gel were subjected to IOBz or CNBr in-gel cleavage as describe above and analyzed in 16.5% tris-tricine SDS-PAGE. All the experiments were reproduced in triplicate.

In analysis of U11 snRNA sites cross-linked to the ^{His6}eS1, the reaction mixture (20 μl) containing 1 μM 4-thiouridine-bearing U11 snRNA and 1 μM ^{His6}eS1 was prepared, incubated and UV-irradiated as above. RNA was recovered from the mixture pretreated with 0.01 mg/ml proteinase K for 10 min at 37°C by phenol–chloroform deproteination and used in the reverse transcription reaction as described above. The resulting products were resolved by 8% denaturing PAGE and autoradiographed as above.

Depletion of rp eS1 in HEK293 cells and RNA level quantification by RNA-seq and real-time PCR

Design of siRNAs against rp eS1 was carried out utilizing Block-iT™ RNAi Designer tool (Thermo Fisher Scientific). Four dsDNA duplexes corresponding to the designed siRNAs were obtained by annealing of the respective oligodeoxyribonucleotide pairs (from 19F/R to 22F/R) and cloned into pSUPER vector (24) to generate plasmids pSUPER_eS1 (#1–4). HEK293 cells were cultured in 60 mm Petri dishes to 70–80% confluence and transfected by a mix of pSUPER_eS1 (#1–4), utilizing TurboFect transfection reagent (Thermo Fisher Scientific). Two days after the transfection, the cells were washed with ice-cold PBS and collected by centrifugation at 1000 *g* for 5 min at 4°C.

Total cellular RNA was isolated using TRIzol reagent (Thermo Fisher Scientific) according to the manufacturer's protocol with subsequent treatment with On-Column DNase I Digestion Set (Sigma) and rRNA depletion with Globin-Zero Gold Kit (Epicentre). Quality of the isolated RNA was controlled on Agilent 2010 Bioanalyzer using RNA 6000 Pico kit (Agilent Technologies). DNA-library was prepared using the SOLiD Total RNA-Seq Kit and RNA Barcoding Kit (Life Technologies) according to the manufacturer's instructions. The sequencing was performed on SOLiD 5500xl platform (Life Technologies). The resulting reads length was 50 or 75 bp. The RNA-seq data were submitted to the GenBank under the study accession number PRJNA337889 and the sample accession numbers SRS2126608–SRS2126613. To minimize sequencing errors, color-space reads were subjected to error correction using SOLiD Accuracy Enhancement Tool v.2.4 (Life Technologies). Corrected data were then analyzed using CLC GW 9.0 (Qiagen) with default parameters. After adapter and quality trimming, SOLiD reads were mapped to hg38 reference genome with Ensemble annotation GRCh38.88. The coordinates of minor introns were obtained from U12DB (25). Minor introns intersecting with any exon sequences were excluded from the analysis.

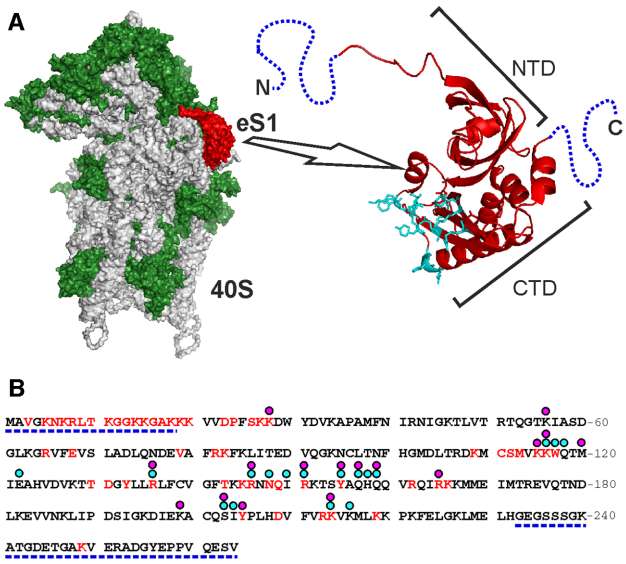

Figure 1. RNA-binding sites of human rp eS1. (**A**) The location of rp eS1 (red) on the human 40S ribosomal subunit (on the left) in the interface view showing 18S rRNA (gray) and ribosomal proteins (green), and the structure of the ribosome-bound protein (on the right) (PDB ID: 4V6X (2)). Amino acids contacting 18S rRNA are shown in cyan; the N- and C-terminal domains are marked with brackets; unresolved protein's fragments are shown as deep blue dashed lines. (**B**) The rp eS1 sequence with amino acid residues involved in RNA binding according to the BindN+ (28) prediction (red letters) and with residues contacting 18S rRNA in the 40S subunit in accordance with human ribosome models with PDB IDs: 4V6X (2) (cyan dots) and 5AJ0 (29) (magenta dots). The rp eS1 fragments unresolved in the models are underlined with deep blue dashed lines.

The cDNA synthesis for quantitative real-time PCR was performed with the use of 1 μg of total RNA (see above), 2.5 μM random $d(N)_6$ primer and 200 U Superscript IV reverse transcriptase (Thermo Fisher Scientific) according to the manufacturer's protocol. Real-time PCR reactions were carried out in a CFX96 thermal cycler (Bio-Rad Laboratories) with the application of SYTO 82 as a fluorescent dye. Primers RNU11_Frt and preRNU11_Rrt were used to quantify the U11 pre-snRNA; GAPDH-specific primers (GAPDH_F and GAPDH_R) were applied to normalize the cDNA. The experiment was reproduced in four biological replicates, each being carried out in technical triplicate.

Rp eS1 and U1 snRNP structure analysis

The PyMol (26) and Chimera (27) software programs were used in analysis of the PDB files. Online BindN+ software (28) was applied for prediction of the rRNA-binding residues of rp eS1 with specificity parameter equal to 90%.

RESULTS

RNA-binding sites in human rp eS1

Cryo-EM structural studies of the human 80S ribosome (2,29) have shown that rp eS1 is located at the platform region of the 40S ribosomal subunit close to the mRNA exit site (Figure 1A). According to ribosome models presented in these studies, the central part of the protein is globular and folded in two weakly interacting domains, the N-terminal (NTD) and C-terminal (CTD), whereas the long N- and C-terminal extensions of the protein remain mostly unresolved and, probably, are intrinsically disordered regions (IDRs). Extensive contacts of 18S RNA with rp eS1 are formed mainly by nucleotides grouped within the CTD (Figure 1A). Using web-based tool BindN+ (28), which defines well enough RNA-binding amino acid residues in protein sequences, we revealed another RNA-binding site within the N-terminal extension of rp eS1 (Figure 1B). Remarkably, this region of the protein is not involved in the interaction with 18S rRNA and, thus, it does not participate in the formation of the ribosome structure. Therefore, the predicted rp eS1 site might provide the implication of the protein in some cellular processes where it operates as an independent player performing a specific function rather than as a structural component of the ribosome.

In-cell RNA cross-linking to rp eS1

To identify the species of RNA that interact *in vivo* with rp eS1, we employed the PAR-CLIP method (21). For this purpose, we obtained stably transfected HEK293-based cell line inducibly producing ^{FLAG}eS1. The plasmid for the cell transfection was prepared using a mammalian expression vector with cloned DNA insert, enabling the expression of the gene of interest in transfected cells in response to DOX treatment (Figure 2A). To ensure that the ectopically produced ^{FLAG}eS1 was functionally active and could replace native rp eS1 in the 40S ribosomal subunit assembly as well as in the course of translation, we performed polysome profiling with subsequent western blot analysis of the sucrose density gradient fractions containing ribosomes and polysomes for the presence of ^{FLAG}eS1. All these fractions were shown to contain ^{FLAG}eS1, implying that the N-terminal FLAG-epitope does not considerably interfere with the protein activity and that ^{FLAG}eS1 functions properly (Figure 2B). We also did not find any significant differences between the profiles of polysomes derived from cells producing ^{FLAG}eS1 and from non-induced cells, suggesting that the endogenous synthesis of ^{FLAG}eS1 in cells had no effect on the general translational level. Nevertheless, we yet observed a noticeable increase in the ^{FLAG}eS1 levels in 80S ribosomes and light polysomes relative to its level in heavy polysomes as compared to those of native rp eS4 taken as a reference (Figure 2B), which indicated that ^{FLAG}eS1-containing ribosomes were somewhat less active in translation than those containing native rp eS1.

To ascertain that the total level of rp eS1 (both endo- and exogenous) in the cells ectopically generating ^{FLAG}eS1 did not differ much from the level of rp eS1 in the non-induced cells, which otherwise might affect the cellular gene expression profile, we estimated the levels of rp eS1 and ^{FLAG}eS1 in transfected cells before and after the induction. Western blotting of the respective cellular lysates revealed that even 3 days after the induction the level of ^{FLAG}eS1 remained much less than that of endogenous rp eS1, and that the level of endogenous rp eS1 practically did not change (Figure 2A, line 2). All this argued that transfected HEK293 cells produced ectopically ^{FLAG}eS1 that could be utilized in PAR-CLIP assay.

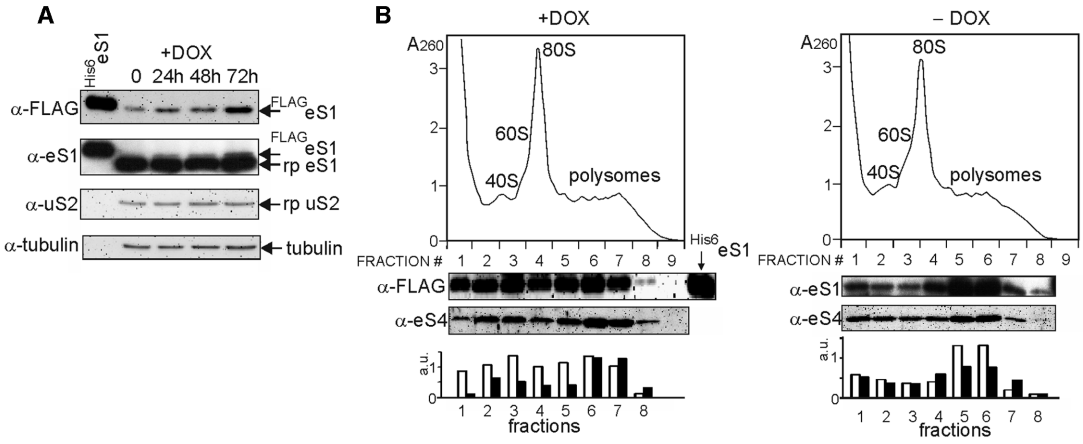

Figure 2. Production of ^{FLAG}eS1 in transfected HEK293 cells and incorporation of the protein into ribosomes. (**A**) Western blot analysis of the ^{FLAG}eS1, rp eS1, rp uS2 and tubulin production in transfected cells after induction by DOX with the use of the antibodies against the respective proteins or FLAG-peptide (designated on the left). Lane ^{His6}eS1, recombinant rp eS1 as a marker. (**B**) The representative profiles of sedimentation in the sucrose gradient of extracts of transfected HEK293 cells induced with DOX (+DOX) and without the induction (−DOX) and western blot analysis of the gradient fractions for the content of ^{FLAG}eS1, rp eS1 and rp eS4 as a 40S subunit protein taken as a control. Gradient fractions are numbered from top to bottom. Diagrams below represent a quantification of the respective western blots (in arbitrary units, a.u.), where the black and white columns correspond to rp eS4 and rp eS1 (exogenous, +DOX or native, −DOX), respectively.

In-cell RNA cross-linking was performed by mild UV-irradiation of DOX-induced cells preliminary treated by 4-thiouridine or 6-thioguanosine. After cell lysis and RNase treatment, both ^{FLAG}eS1 bearing covalently attached RNA moieties and the free protein were isolated with the use of anti-FLAG antibodies immobilized on magnetic beads with the subsequent ^{32}P-labeling of the cross-linked RNA fragments followed by their isolation by denaturing SDS-PAGE. To avoid contamination of the RNA-^{FLAG}eS1 cross-links by free RNA fragments, which in a large amount co-migrated at the same gel region as the cross-links, the latter were transferred onto a nitrocellulose membrane and detected by autoradiography. Preliminary SDS-PAGE analysis of the aliquoted samples together with the following transferring of the cross-links onto nitrocellulose and western blotting showed that RNA-^{FLAG}eS1 cross-links migrated in the gel as a broad band above that of unmodified rp eS1 (Figure 3A). Noticeably, the 4-thiouridine-treated cells produced much more cross-linked RNA than the cells treated with 6-thioguanosine, implying either a higher efficiency of 4-thiouridine-containing RNA cross-linking or an enrichment of rp eS1 binding sites in RNA with uridines (Figure 3A). Therefore, only 4-thiouridine-generated RNA-^{FLAG}eS1 cross-links eluted from membrane after its treatment by proteinase K were further subjected to NGS analysis.

NGS data analysis of RNA fragments cross-linked to ^{FLAG}eS1

Analysis of the NGS data obtained with the RNA fragments cross-linked to ^{FLAG}eS1 revealed a vast number of sequencing reads corresponding to rRNA (which was expected) and reads related to other types of cellular RNAs (see 'Materials and Methods' section). The former were eliminated from next rounds of analysis because the information on the contacts of rp eS1 with rRNA in human ribosome is available. To identify other kinds of RNAs cross-linked to ^{FLAG}eS1, we mapped the remaining reads to the human genome using CLC GW 9.0 software and afterward we picked up the reads that formed the locally distributed peaks with a characteristic shape and significant coverage. Genomic regions corresponding to the particular cross-linked RNA fragments were determined on distinctive T/C transitions in the reads, which were absent in the control experiment with 4-thiouridine-untreated cells. These transitions are known to arise because reverse transcriptase used in the library preparation is unable to recognize cross-linked 4-thiouridine residues as uridines, taking them as cytidines (21). Selecting peaks containing T/C transitions, we identified several genes (Supplementary Table S2) and two of them, *RNU5A-1* and *RNU11* genes, displayed particularly high level of such transitions (Supplementary Figure S1 and Table S2). The former encodes the U5 snRNA (30) functioning in both the major and minor class spliceosomes (31), whereas the latter corresponds to the minor class spliceosome component, U11 snRNA, whose level in cells is much lower as compared to those observed for the major-class spliceosome snRNAs (31). Remarkably, T/C transitions in the reads corresponding to these genes were not at discrete locations but were spread along the sequences within the T-rich regions without evident consensus (Supplementary Figure S1). The mapping of the 4-thiouridine residue positions corresponding to the most frequently occurring T/C transitions onto the snRNA structures revealed that they match to uridines located mostly in the single-stranded region of U11 snRNA containing the Sm site and in the apical Loop 1 of U5 snRNA (Figure 3B). Since T/C transitions indicate the existence of cross-links between 4-thiouridine residues in RNA and protein contacting them, we concluded that the interactions of ^{FLAG}eS1 with the above-mentioned regions of RNAs transcribed from the U11 and U5 snRNA-encoding genes took place in living cells.

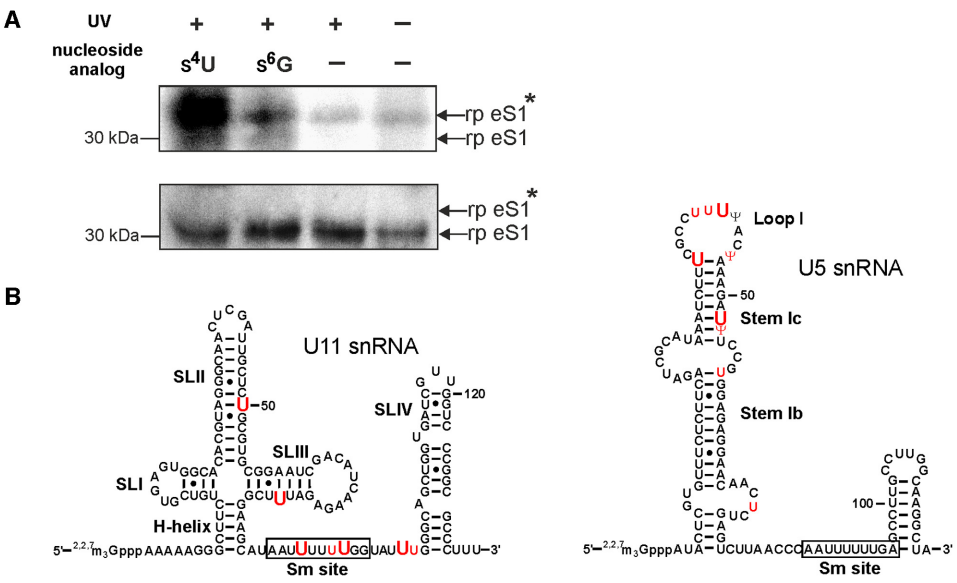

Figure 3. In-cell rp eS1 cross-links found by photoactivatable-ribonucleoside-enhanced cross-linking and immunoprecipitation (PAR-CLIP). (**A**) Autoradiograph of membrane with transferred onto it ^{FLAG}eS1-RNA cross-links separated by sodium dodecyl sulfate polyacrylamide gel electrophoresis (SDS-PAGE) (upper panel); western blot analysis of the same membrane using anti-rp eS1 antibodies (lower panel). Arrows indicate positions of unmodified rp eS1 and cross-linked ^{FLAG}eS1 (designated as rp eS1*). The cross-links were isolated from cells grown on either 4-thiouridine (4sU) or 6-thioguanosine (6sG) or without the nucleoside analog (−) and either irradiated (+) or not irradiated (−) with UV light. (**B**) The secondary structures of human U11 and U5 snRNAs (40) with the indication of the uridines (red) corresponding to the positions of T/C transitions; positions of the most frequent (>5%) transitions are shown by enlarged letters.

It is known that the Sm site is present in the structure of almost all RNAs transcribed from the U snRNA-encoding genes, but in mature snRNPs this site is occupied by a group of seven proteins called Sm proteins (32), which associate with pre-snRNAs during the cytoplasmic phase of the snRNP assembly (33,34). Processed snRNAs being complexed with the Sm proteins are then imported into the nucleus where they undergo post-transcriptional modification (33). Therefore, it seems unlikely that rp eS1 is bound to the Sm site of mature U11 snRNA, but the protein could interact with this site before processing of U11 pre-snRNA. Interestingly, rp eS1 was associated with RNA encoded by the *RNU5A-1* gene via a structural element other than the Sm site (see above).

Immunoprecipitation of rp eS1-containing snRNPs from HEK293 cell extracts

The assumption that rp eS1 could interact with the unprocessed U11 pre-snRNA was a motivation for determining whether rp eS1 is bound to U11 pre-snRNA in the nucleus where this RNA is synthesized, or in the cytoplasm, where its 3′-end processing occurs. Therefore, we performed immunoprecipitation of RNPs from nuclear and cytoplasmic extracts of HEK293 cells using anti-rp eS1 antibodies and determined the U11 pre-snRNA content in the respective samples of total RNA co-precipitated with rp eS1 by RT-PCR assay. Since one of the PCR primers used in the analysis matched a site in the mature U11-snRNA, and the second was complementary to a site located in the U11 pre-snRNA region undergoing 3′-end processing, the mature U11 snRNA could not be detected in this way, while U11 pre-snRNA was found to be associated with rp eS1 in both the nucleoplasm and the cytoplasm (Figure 4A). This finding suggests that rp eS1 binds to U11 pre-snRNA in the cell nucleus and then it is exported into the cytoplasm in the respective complex. To determine whether rp eS1 remains associated with the mature U11 snRNA imported into the nucleus after the U11 pre-snRNA processing, we performed a similar RT-PCR analysis with total RNA co-precipitated with rp eS1 from nuclear extract using two pairs of primers specific for the U11 and U12 snRNAs. It should be noted that the use of only U11 snRNA-specific primes could not be informative in this analysis, because the U11 snRNA sequence is entirely represented in U11 pre-snRNA. Therefore, considering that nuclear U11 snRNP exists as U11/U12 di-snRNP (35,36), it seemed reasonable to determine the content of U12 snRNA in a sample of total RNA co-precipitated with rp eS1 from nuclear extract to find out whether U11 snRNA is contained therein. As can be seen in Figure 4B, both U11 and U12 snRNAs were co-precipitated with rp eS1 from the nuclear extract, implying that rp eS1 remains bound to the mature U11 snRNA even when the latter operates in splicing. Surprisingly, no specific signal was detected when the total nuclear rp eS1-bound RNA was analyzed in the same way using primers specific for the U5 snRNA/U5 pre-snRNA (Figure 4C), indicating that there were no stable rp eS1 complexes with these RNAs, which could be detected by immunoprecipitation with anti-rp eS1 antibodies. Therefore, we further focused on studying the interaction of rp eS1 with U11 snRNA.

Binding of rp eS1 to U11 snRNA T7 transcripts

The occurrence of the rp eS1 cross-linking sites in RNA sequences present in both mature U11 snRNA and its pre-

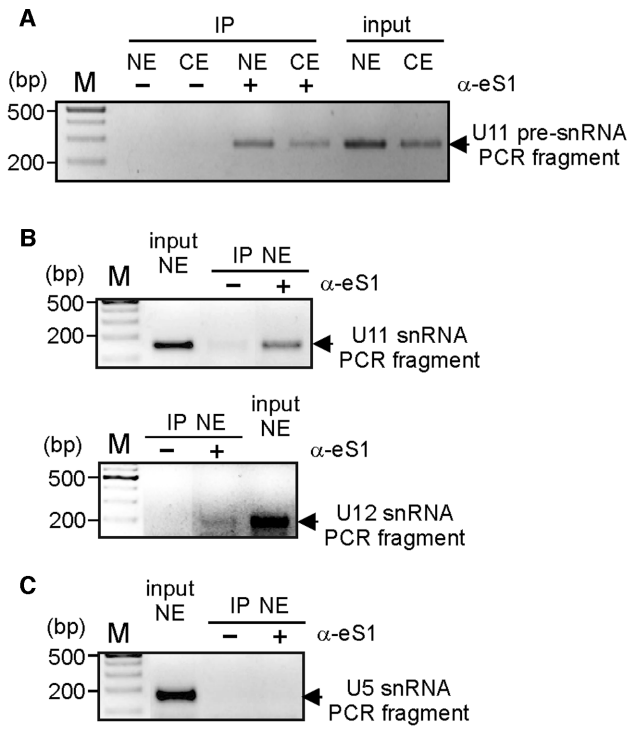

Figure 4. Immunoprecipitation of snRNAs from HEK293 cell extracts using anti-rp eS1 antibodies (α-eS1). Reverse transcriptase polymerase chain reaction (RT-PCR) analysis of the RNA co-immunoprecipitated (IP) from the nuclear (NE) and cytoplasmic (CE) extracts with beads bearing immobilized α-eS1 (+) and empty beads (−) followed by electrophoretic separation of the PCR products on an agarose gel. Positions of the PCR products obtained with primers specific for the fragments of U11 pre-snRNA (panel **A**), U11 and U12 snRNAs (panel **B**) and U5 snRNA (panel **C**) marked by arrows. Input, cDNA synthetized on the samples of the total RNA isolated from the nuclear or cytoplasmic cell extracts.

cursor together with the lack of these sites in sequence corresponding to the U11 pre-snRNA part eliminated during processing prompted us to test the ability of rp eS1 to bind *in vitro* to isolated U11 snRNA. To do this, ^{32}P-labeled snRNA T7 transcript further referred to as U11 snRNA and ^{His6}eS1 were utilized. The affinity of ^{His6}eS1 for U11 snRNA determined by NCFBA turned out to be rather high ($Ka = 3.8 \pm 1.2 \times 10^7$ M^{-1}) (Figure 5A). Considering that ribosomal proteins bearing a high positive charge are usually prone to the formation of non-specific aggregates with RNA (37,38), we examined the ^{His6}eS1 binding to U11 snRNA using EMSA allowing the visualization of bound and unbound RNA as well as aggregates precipitated in the gel wells. ^{His6}eS1 was found to be capable of retarding the mobility of U11 snRNA in the gel, resulting in the appearance of two differently migrating bands (Figure 5B), which most likely corresponded to complexes possessing different structures.

To learn whether the Sm site region contributes to the U11 snRNA interaction with rp eS1, we investigated the binding of ^{His6}eS1 to U11 snRNA(ΔSm), which lacks a 3′-terminal fragment comprising the Sm site and besides, we also examined inhibitory effect of $(pU)_8$ on the binding of the protein to U11 snRNA. It was found that *Ka* ($1.3 \pm 0.4 \times 10^7$ M^{-1}) for binding of U11 snRNA(ΔSm) to ^{His6}eS1 was one third of the value determined for the full-length U11 snRNA (Figure 5A) and that unlike U11 snRNA, U11 snRNA(ΔSm) bound to^{His6}eS1 was manifested in the gel by EMSA as a single band, indicating the existence of another portion of rp eS1 binding site in U11 snRNA, which is most likely the main one, in addition to the portion in the U-rich region (Figure 5C). The results on the binding of ^{His6}eS1 to U11 snRNA(ΔSm) are consistent with those obtained with $(pU)_8$ as a competitive inhibitor of the binding of U11 snRNA to ^{His6}eS1. In particular, as revealed by NCFBA, $(pU)_8$ only partially displaced ^{His6}eS1 from the complex with U11 snRNA (Figure 5D), which according to EMSA was accompanied by a decrease in the intensity of the more slowly migrating complex band, while the intensity of the faster migrating band did not change (Figure 5E). Therefore, the slowly migrating band can be attributed to the complex, in which the Sm-site containing U-rich region of U11 snRNA is involved in the interaction with the protein, while the faster migrating band likely corresponds to the complex where this region does not participate in the binding. As expected, $(pU)_8$ did not affect the binding of U11 snRNA(ΔSm) to ^{His6}eS1 (Figure 5F). Thus, the obtained results indicate that the U-rich sequence in U11 snRNA is not the primary binding site of ^{His6}eS1, although this sequence contributes significantly to the protein binding. Remarkably, U11 snRNA was unable to bind to 40S ribosomal subunits (Figure 5A), suggesting that the rp eS1 site responsible for the protein binding to this RNA either is hidden in the spatial structure of the 40S ribosome or its fold is inappropriate to ensure the binding.

Region of U11 snRNA involved in rp eS1 binding

To outline the RNA regions involved in the rp eS1 binding, we performed footprinting of U11 snRNA complexed with ^{His6}eS1 using CMCT as a probe specific to the N3 of unpaired uridines and in a lesser extent to the N1 of guanosines (39). In addition, to reveal the rp eS1-dependent changes in the accessibility of U11 snRNA nucleotides, we applied hydroxyl radicals that attack exposed C4′ atoms of riboses, causing cleavages in the RNA backbone (40) and BzCN that selectively interacts with 2′-OH groups of riboses (41). The U11 snRNA nucleotides modified by BzCN or CMCT in the presence or absence of ^{His6}eS1 together with the positions, by which cleavages by hydroxyl radicals occurred, were determined by extension of ^{32}P-labeled primer on the isolated RNA in the reverse transcription reactions followed by separation of the reaction products by electrophoresis in denaturing PAGE.

We found that the ^{His6}eS1 binding to U11 snRNA resulted in the protections of the nucleotides of SLI (G14, U15 and U18), SLIII (C62, C65, U67 and C68), the Sm site-containing single stranded region (U86, G96, U97 and A98) and H-helix (C84) adjacent to this region from the attack of hydroxyl radicals (Figure 6A and C). In addition, the protections of nucleotides U18, U22 and U86 from the modification with CMCT and of nucleotides U18, G83 and C84 from the BzCN attack were revealed (Figure 6B and C). These nucleotides belong to SLI (U18 and U22) and to the H-helix (G83, C84 and U86) mentioned above. The

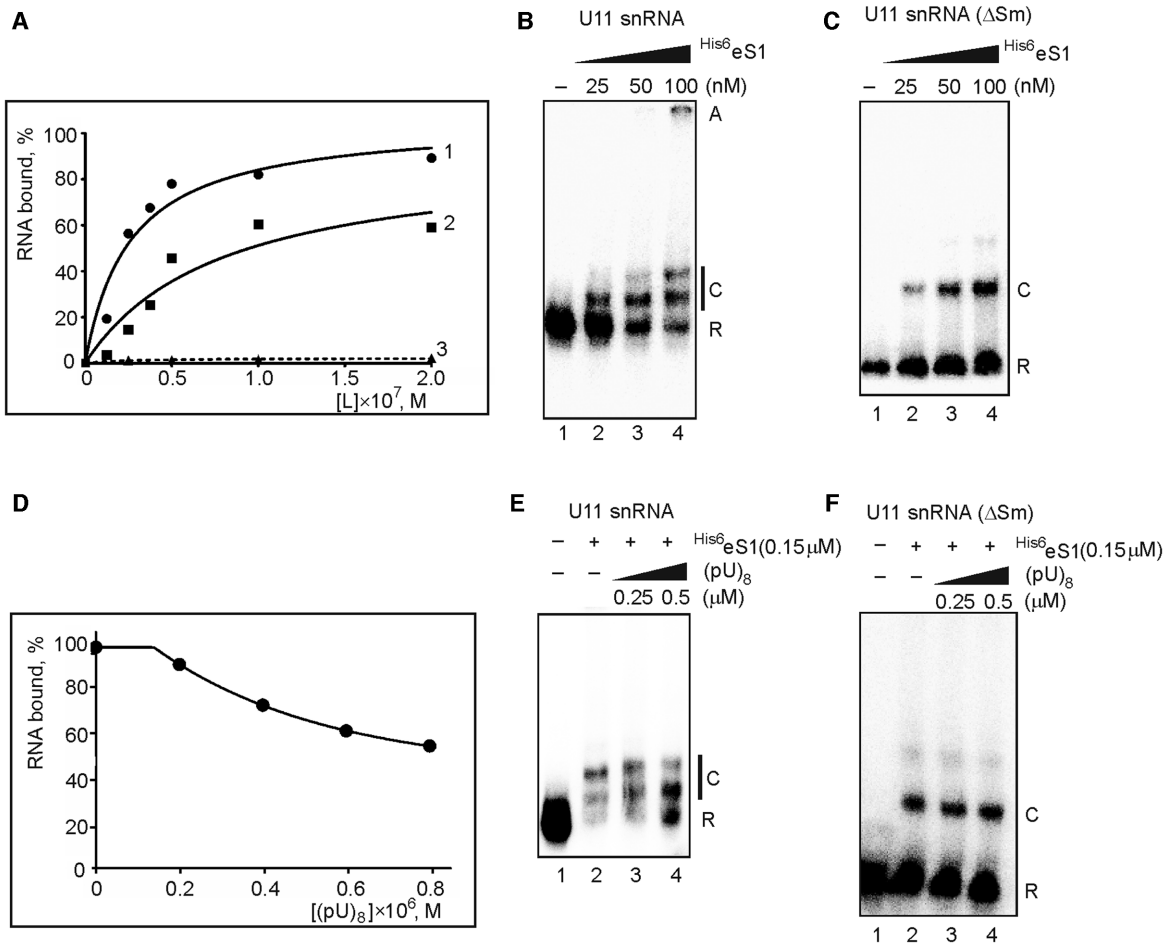

Figure 5. Binding of ^{32}P-labeled snRNA T7 transcripts to ^{His6}eS1 and human 40S ribosomal subunits. (**A**) The binding isotherms of U11 snRNA to ^{His6}eS1 (1) and to 40S ribosomal subunits (3) and of U11 snRNA(ΔSm) to ^{His6}eS1 (2) measured by NCFBA. The error in the measurements was within 30%. EMSA of the complexes of ^{His6}eS1 (in the indicated concentrations) with U11 snRNA (**B**) and with U11 snRNA(ΔSm) (**C**). Positions of free RNAs (R), their complexes with ^{His6}eS1 (C) and aggregates (A) are indicated on the left. (**D**) Inhibitory effect of $(pU)_8$ on ^{32}P-labeled U11 snRNA binding to ^{His6}eS1 (0.15 μM) measured by NCFBA. EMSA of the complexes of ^{His6}eS1 (0.15 μM) with U11 snRNA (**E**) and U11 snRNA(ΔSm) (**F**) formed in the presence of $(pU)_8$.

protections observed with U11 snRNA in the presence of ^{His6}eS1 indicate that the respective RNA regions are either involved in the formation of the rp eS1 binding site or located in close proximity to it. At the same time, ^{His6}eS1-bound U11 snRNA region 87–100 comprising the U-rich sequence, where the Sm site is located, exhibited the strongly enhanced accessibility to BzCN (Figure 6B and C), which implies the extensive protein-dependent rearrangements in the backbone of this region; besides, G53 residing close to SLIII displayed the increased accessibility to hydroxyl radicals (Figure 6A and C).

Based on the footprinting data, we attempted to imagine the arrangement of the rp eS1 binding site on U11 snRNA, comparing it to the location of the corresponding site on the 18S rRNA in the 40S ribosomal subunit where rp eS1 appears in the cleft between 18S rRNA helices (h) 22 and 26 that contact the protein (Figure 7). Since the spatial structure of U11 snRNA is unknown, we used instead a structure of its homolog, U1 snRNA, in U1 snRNP (42). Remarkably, the spatial structure of U1 snRNA also has a cleft between SLI and SLIII, although its SLI is significantly longer than SLI in U11 snRNA. We believe that in general, the architecture of the U11 snRNA region comprising SLI and SLIII is similar to that of the 18S rRNA region containing h22 and h26 (Figure 7). It should be noted that the Sm site-containing strand in the model of the U1 snRNA spatial structure in U1 snRNP is located rather apart from SLI and SLIII; however in free U1 snRNA, this strand should be certainly flexible and could approach these SLs. Therefore, considering ^{His6}eS1-dependent protections of nucleotides in SLI and SLIII of U11 snRNA, we conclude that rp eS1 binding site is located in the cleft between the above SLs, mimicking the respective site on the 18S rRNA in the 40S ribosomal subunit, and that this site is the primary binding region of rp eS1 on the U11 snRNA.

U11 snRNA cross-linking site in rp eS1

To determine the portion of rp eS1 directly interacting with the U11 snRNA, the cross-linking of ^{His6}eS1 to the ^{32}P-labeled RNA containing randomly incorporated 4-

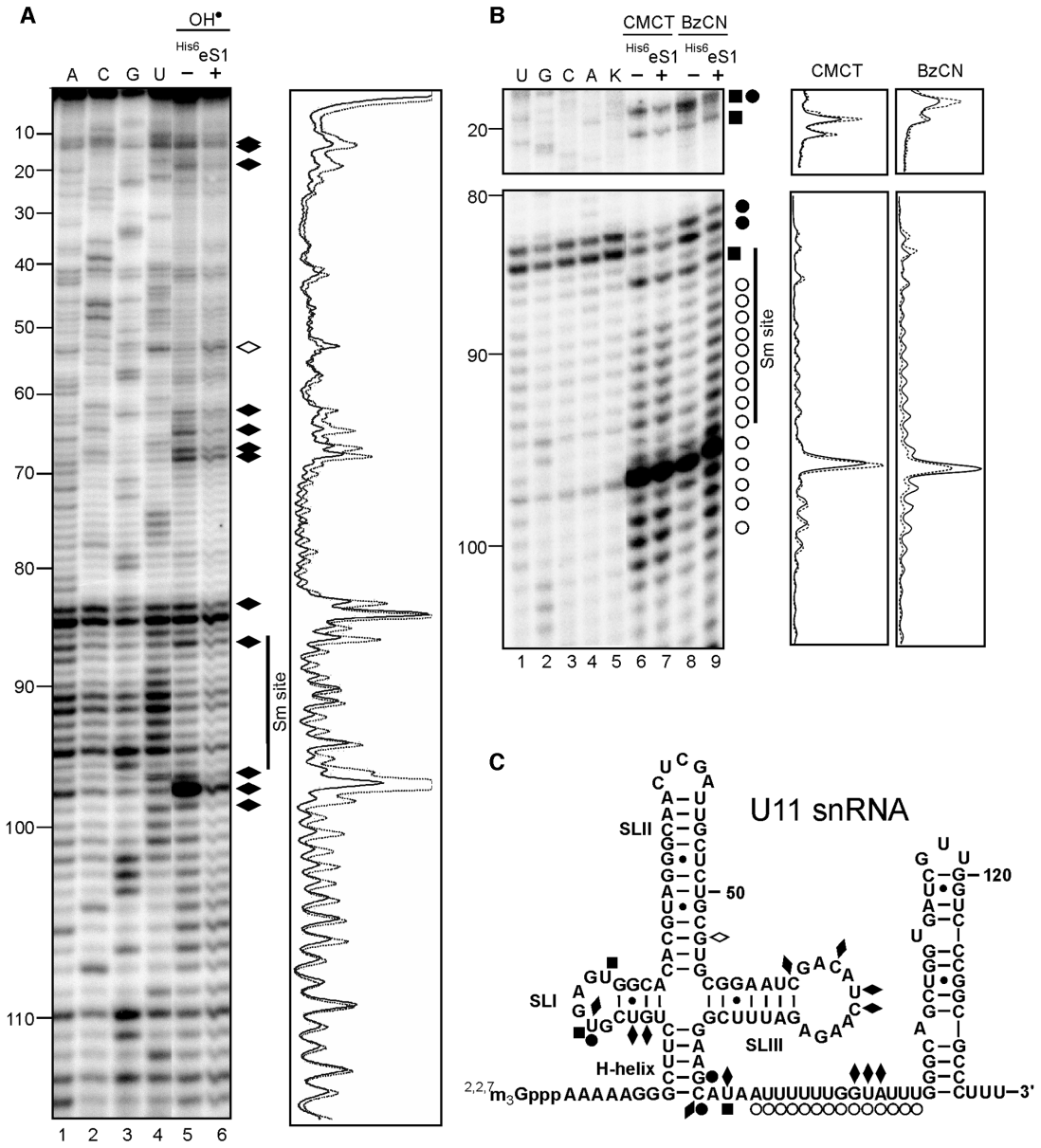

Figure 6. Chemical footprinting of U11 snRNA T7 transcript complexed with ^{His6}eS1. (**A**) Gel autoradiograph after the separation of the reverse transcription products obtained with free RNA (–) and with RNA in a complex with ^{His6}eS1 (+) treated with hydroxyl radicals, and the data of the densitometric analysis corresponding to the lanes '+' (solid line) and '–' (dashed line). (**B**) The same with 1-cyclohexyl-(2-morpholinoethyl)carbodiimide metho-p-toluene sulfonate (CMCT) and benzoyl cyanide (BzCN). On the panels A and B on the right from autoradiographs, positions of protections and enhancements for the nucleotides, whose signal intensity is changed not <1.5-fold after the treatment of a complex with probes, are indicated by the filled and open symbols, respectively (hydroxyl radicals, diamonds; CMCT, squares; BzCN, circles). U, G, C, A—sequencing lanes; K—free untreated RNA. Position corresponding to the Sm site is indicated by a line. (**C**) Mapping of the footprinting data onto the U11 snRNA secondary structure (symbols are the same as on the panels A and B).

thiouridine residues in the respective binary complex was applied with subsequent cleavage of the purified cross-linked protein with site-specific proteolytic agents followed by identification of the fragments bearing the ^{32}P label. To ensure that the complex of ^{His6}eS1 with 4-thiouridine-containing U11 snRNA adequately simulated the state of the respective complex *in vivo*, we identified also the cross-linking sites in the RNA by the primer extension analysis as mentioned above. It was found that most of the 4-thiouridine residues generating RNA–protein cross-links in the binary complex were located at the same positions of U11 snRNA as the residues that were cross-linked to rp eS1 in cells according to our PAR CLIP data (Supplementary Figure S2), which implied that the same protein region provided *in vivo* and *in vitro* cross-linking. For the site-specific cleavage of ^{His6}eS1, CNBr, IOBz and protease ArgC specific to methionine, tryptophan and arginine residues, respectively, were utilized. In the course of the analysis, ^{His6}eS1 cross-linked to U11 snRNA was purified by SDS-PAGE with prior RNase T1 treatment (Figure 8A), and

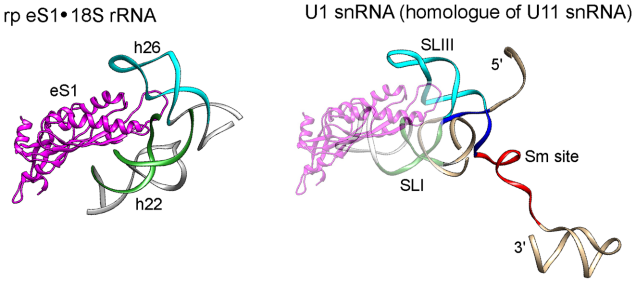

Figure 7. Comparison of the structures of the rp eS1 binding site on the18S rRNA and of U1 snRNA, homolog of U11 snRNA. On the left, the fragment of the structure of the human 40S ribosomal subunit containing helices (h) 22 and 26 and rp eS1 (magenta) (PDB ID: 4UG0) (3). On the right, the fragment of the structure of U1 snRNA in U1 snRNP (PDB ID: 3CW1) (42) where the area corresponding to the rp eS1 binding site on U11 snRNA is designated in light magenta. The fragment of SLI, which lacks a homologous region in U11 snRNA, is colorless. Matching helices are shown in cyan and green. The region of the Sm site and H-helix are shown in red and blue, respectively.

the protein bands were excised from the gel and digested with the proteolytic agents in separate reactions; the products of digestion were resolved on tris-tricine gel followed by autoradiography (Figure 8B). It is seen that the fragments of ^{His6}eS1 bearing the cross-linked RNA moieties migrate in the gel as a broad band corresponding to the products with average molecular masses 10, 8 and 6 kDa for IOBz-, CNBr- and ArgC-cleavage, respectively. When identifying the cross-linking site in the protein, we considered that the RNA moieties remaining covalently attached to the peptides decrease their mobility in the gel. Because the ^{His6}eS1 has two tryptophan residues, its cleavage with IOBz should lead to the formation of three fragments with theoretical molecular masses of 16 765, 9884 and 6489 Da (Figure 8E); therefore, the radioactive band of 10 kDa (Figure 8B) could correspond to the locations of 9884 or 6489 Da IOBz-cleavage fragments. It is seen that 6489 Da fragment overlaps with two CNBr- and three ArgC-cleavage fragments (Figure 8E), from which only the largest ones (5071 Da for CNBr-cleavage and 3853 Da for ArgC- cleavage) could correspond to the cross-linked fragments with masses of 8 and 6 kDa (Figure 8B), respectively. Finally, 9884 Da IOBz-cleavage fragment overlaps with the 7285 Da CNBr-cleavage one (Figure 8E), but these fragments cannot be attributed to the cross-linked fragments of 10 and 8 kDa, since they do not overlap with the 3853 Da ArgC-cleavage fragment that could correspond to the 6 kDa cross-linked one. Thus, the cross-linking site is to be located within a peptide present in the IOBz-, CNBr- and ArgC-cleavage fragments with molecular masses of 6489, 5071 and 3853 Da (Figure 8E), respectively. However, the cross-linking to the 9884 Da IOBz-cleavage fragment cannot be ruled out because ArgC protease might miss the cleavage site(s) in the area corresponding to this fragment. To be sure that attachment of ^{His6}eS1 occurred actually to the 6489 Da IOBz-cleavage fragment, we performed successive cleavage of the cross-linked protein, initially with CNBr and then with IOBz (Figure 8C). With this cleavage, the mobility of the labeled peptide in gel was slightly increased as compared to that observed in CNBr-cleavage alone, which could be only if the cross-linking site was in the CNBr-produced peptide with mass of 5071 rather than of 7285 Da (Figure 8E). In other variants of successive cleavage of the cross-linked protein, initially with ArgC and then with IOBz or CNBr (Figure 8D), the mobility of the labeled peptide was also increased compared with those detected for IOBz- or CNBr-cleavage alone, indicating the location of the cross-linking site within the 3853 Da ArgC-produced peptide (Figure 8E). Thus, we concluded that the cross-linking site in the protein is located in the NTD within peptide 9-LTKGGKKGAKKKVVDPFSKKD-29 enriched with lysines and that this peptide is cross-linked to RNAs transcribed from *RNU5A-1* and *RNU11* genes in cells (see above). Notably, no cross-linking of rp eS1 to 4-tiouridine-containing ^{32}P-labeled U11 snRNA was observed when ^{His6}eS1 was replaced by the human 40S ribosomal subunits (data not shown), confirming that the peptide 9–29 of rp eS1 is involved in the above-mentioned interactions only when the protein is ribosome-free. Remarkably, the identified rp eS1 peptide overlaps the region 5–20, which was predicted as an RNA binding site appeared in addition to the existing 18S rRNA binding site (Figure 1B).

Determination of the functional assignment of the rp eS1 biding to U11 snRNA in cells

Rp eS1 has not been found as a component of both U11 snRNP (43) and complexes of the major-class spliceosome (44), which may mean that it is not a component of mature U11 and U5 snRNPs. But on the other hand, it may have been lost during experimental procedures related to the complex purification and the sample preparation for analysis. Therefore, to reveal a possible functional manifestation of the rp eS1 binding to RNAs transcribed from the *RNU5A-1* and *RNU11* genes, we depleted HEK293 cells of rp eS1 using a set of plasmids (pSuper_eS1_#1–4) generating rp eS1-specific shRNAs (Figure 9A) followed by the comparison of the RNA-seq data for the depleted and non-depleted cells. With rp eS1-depleted cells, the portion of reads covering the genome region 3′ to *RNU11*, which corresponds to the 3′-terminal sequence of the unprocessed U11 pre-snRNA, was significantly higher than that with non-depleted cells (Figure 9B, upper panel). The relative normalized coverage of this region of the genome for rp eS1-depleted cells was much larger than that with non-depleted cells (Figure 9B, lower panel). At the same time, the coverage of the region corresponding to the mature U11 snRNA was reduced, indicating a decreased level of this snRNA in depleted cells (Figure 9B). No significant changes were observed for genes encoding any other snRNAs, including the *RNU5A-1* gene. Quantitative real-time PCR analysis of U11 pre-snRNA levels in rp eS1-depleted and non-depleted cells showed that the level of the U11 snRNA precursor in depleted cells was approximately twice as higher as that in non-depleted cells (Figure 9C). All this strongly suggests that rp eS1 affects the maturation of U11 pre-snRNA, contributing to its 3′-end processing.

Given the diminished level of mature U11 snRNA in rp eS1-depleted cells, it was reasonable to expect also a decrease in the efficiency of splicing of the minor class introns. Analyzing RNA-seq data for depleted and non-depleted

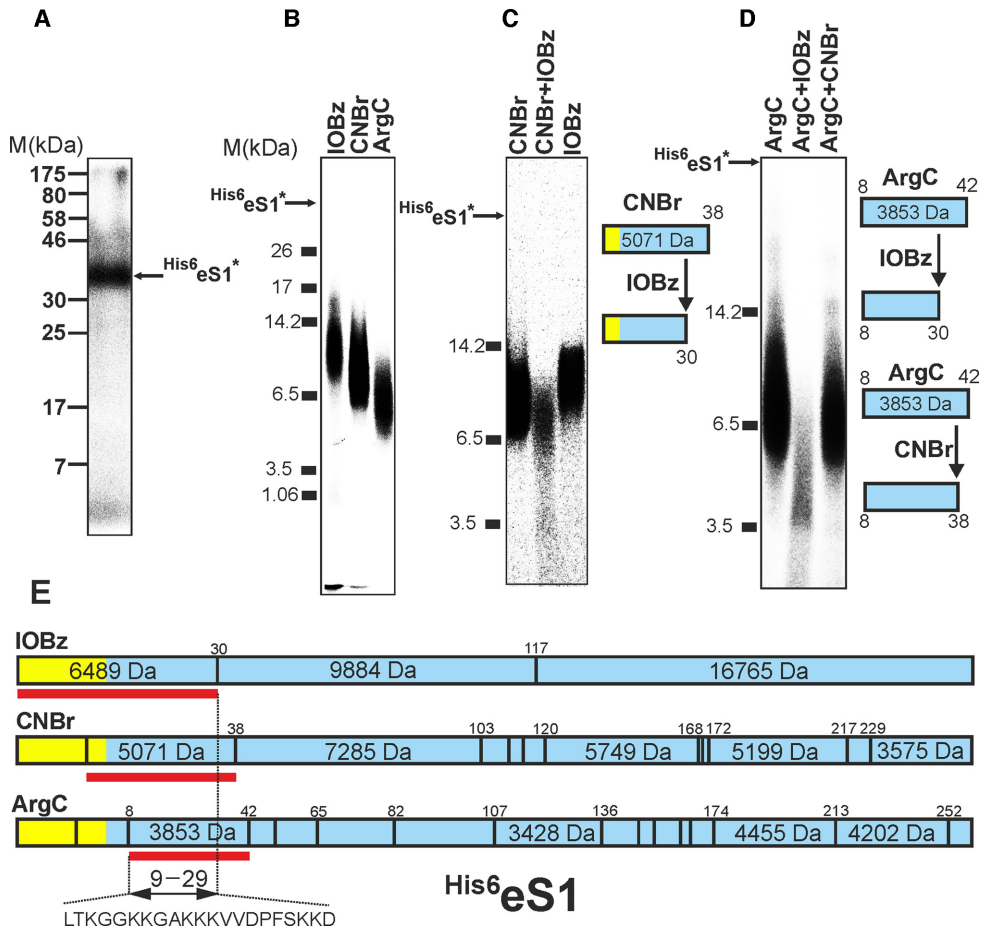

Figure 8. Identification of the rp eS1 fragment cross-linked to ^{32}P-labeled U11 snRNA. (**A**) Isolation of the cross-linked ^{His6}eS1 (^{His6}eS1*) after RNase T1 treatment by SDS-PAGE. (**B**) Separation of the products of cross-linked ^{His6}eS1 digestion with iodosobenzoic acid (IOBz), cyanogen bromide (CNBr) and ArgC in tris-tricine SDS-PAGE. Positions of the protein molecular mass markers and ^{His6}eS1* are shown on the left. (**C** and **D**) Sequential digestion of the cross-linked protein with proteolytic agents and analysis of the obtained products by SDS-PAGE. Positions of the protein molecular mass markers are shown on the left. Schematic representation of the labeled peptides resulting from the sequential digestion of the cross-linked ^{His6}eS1 is given on the right. (**E**) Maps of the digestion of ^{His6}eS1 (containing both His_6 and FLAG tags) with the proteolytic agents where calculated molecular masses of the resulted peptides are indicated; regions corresponding to the native rp eS1 and those conforming to the N-terminal protein tag containing His_6 together with FLAG are colored in blue and yellow, respectively. Peptides found as bearing the ^{32}P-labeled RNA fragments are underlined. The sequence of cross-linked peptide confined with dashed lines is presented.

cells, we did indeed found a substantial reduction in the splicing efficiency of such introns in rp eS1-depleted cells compared to that in non-depleted cells. In particular for the first nine minor intron-containing genes with the highest read coverage (i.e. value of RPKM, reads per kilobase per million mapped reads), the ratio of the coverage of the minor introns to the coverage of all (major and minor) introns for the same gene in rp eS1-depleted cells was on average 38% higher than in non-depleted cells (Figure 9D).

DISCUSSION

In this study, applying PAR-CLIP method to HEK293 cells and utilizing 4-thiouridine as a photoactivatable ribonucleoside, we demonstrated for the first time that rp eS1 is involved in functional interactions with RNAs other than ribosomal ones. The NGS analysis showed that this protein cross-linked to RNAs corresponding to transcripts of the U11 and U5 snRNA-encoding genes. The protein cross-linking sites were mostly located in sequences that match to the Sm site-containing U-rich single-stranded region of U11 snRNA and to the apical part of Loop I of U5 snRNA. It was found that rp eS1 is associated with U11 pre-snRNA both in the nucleus and in the cytoplasm, and that rp eS1 is also bound to U11/U12 di-snRNP operating in splicing, whereas rp eS1 complexed with U5 snRNA/U5 pre-snRNA was not detected. *In vitro* binding of recombinant rp eS1 to T7 transcripts corresponding to U11 snRNA and its truncated form, U11 snRNA(ΔSm), which lacks a 3′-terminal fragment comprising the Sm site, revealed that the *Ka* value for U11 snRNA(ΔSm) is reduced by 3-fold compared to that for full-length U11 snRNA. Besides, the binding level of the U11 snRNA to rp eS1 was considerably decreased in the presence of $(pU)_8$ as a competitive inhibitor of the binding of the above U-rich region to rp eS1. All this confirms the involvement of the Sm site-containing U-rich region of U11 snRNA in specific interaction with rp eS1. Applying the chemical footprinting of U11

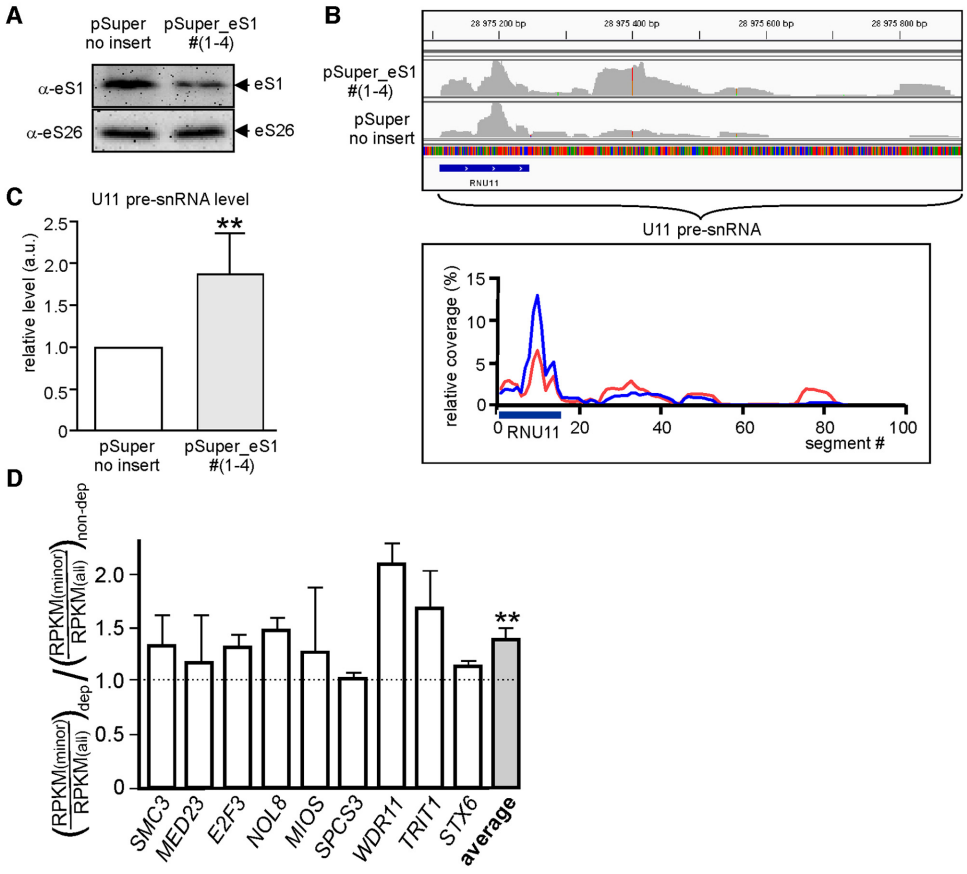

Figure 9. Effects of the rp eS1 depletion in HEK293 cells. (**A**) Western blot analysis of the rp eS1 and rp eS26 (a 40S ribosomal subunit protein taken as a control) in HEK293 cells transfected with either the set of four plasmids generating shRNAs against rp eS1 mRNA (pSuper_eS1_#(1–4)) or empty vector (pSuper_no insert). The antibodies used are indicated on the left. (**B**) The representative fragment of the IGV genome browser view (upper panel) showing the read coverage of the range corresponding to U11 pre-snRNA (designated by a brace) in human genome after next generation sequencing (NGS) analysis of the total RNA isolated from cells depleted of rp eS1 (pSuper_eS1_#(1–4)) and non-depleted cells (pSuper_no insert). The relative normalized coverage (lower panel) in the genome range corresponding to U11 pre-snRNA for cells depleted of rp eS1 (red line) and non-depleted cells (blue line) (obtained from two biological replicates). Blue bar designates the genome region for mature U11 snRNA. (**C**) Quantitative real-time PCR analysis of the U11 pre-snRNA level in cells depleted of rp eS1 (pSuper_eS1_#(1–4)) relatively that in non-depleted cells (pSuper_no insert). Error bars represent S.D. from four biological replicates; $^{**}P < 0.005$, two-tailed Student's *t*-test; a.u., arbitrary units. (**D**)Read coverage of the minor introns normalized to that of all introns in the gene calculated from RNA-seq data obtained with rp eS1-depleted cells relatively that with non-depleted cells. Results for nine genes containing minor introns and displaying maximum reads per kilobase per million mapped reads (RPKM) of introns are presented. Error bars are S.E.M. from three biological replicates; $^{**}P < 0.01$, same as above.

snRNA bound to rp eS1 with the use of hydroxyl radicals, CMCT and BzCN as probes of different specificity, and a site-directed cross-linking approach utilizing 4-thiouridine-containing U11 snRNA, we obtained comprehensive information on distinctive features of the interaction of U11 snRNA with rp eS1. It was found that rp eS1 bound to U11 snRNA protects from modification nucleotides in SLI and SLIII as well as in the U-rich single-stranded sequence where the Sm site is located, and in H-helix adjacent to this sequence. In addition, extensive rp eS1-induced rearrangements were revealed in the backbone of the Sm site region of U11 snRNA. The N-terminal K-rich region 9–29 of rp eS1 was found to be responsible for the protein interaction with the aforementioned U-rich region of U11 snRNA both *in vitro* and *in vivo*. It turned out that in living cells, rp eS1 is bound to U11 pre-snRNA both in the nucleus and in the cytoplasm. But when the cells were depleted of rp eS1, the level of non-processed U11 pre-snRNA significantly increased and the efficiency of splicing of minor class introns decreased. In general, our findings provide new information on the functions of human ribosome-unbound rp eS1, indicating its implication in cellular events related to the biogenesis of U11 snRNA and to minor class splicing.

U11 snRNA is a component of the low-abundant minor spliceosome, which is responsible for the excision of rare U12-type introns during pre-mRNA splicing (35). It is known that a multicomponent complex containing the survival of motor neuron (SMN) protein, gemins 2–8 and several other proteins, the so-called SMN complex, initiates the cytoplasmic maturation phase of all snRNPs, including U11 snRNP (33,34). The SMN complex ensures the assembly of Sm proteins into a core structure around the Sm site of pre-snRNAs. The data obtained in this study allow us to suggest that rp eS1 binds to U11 pre-snRNA in the nucleus, and then it is exported to the cytoplasm in a complex with this RNA. The binding of rp eS1 causes re-

arrangement of U11 pre-snRNA in the Sm site region, as revealed from the footprinting results with T7 U11 snRNA transcript. Restructuring of this region may be required to provide interaction of the RNA with the Sm protein-bound SMN complex in the cytoplasm. Obviously, before Sm protein binding, the Sm site should be free from the rp eS1 N-terminal IDR that interacts with the region containing Sm site upon association of rp eS1 with the U11 pre-snRNA. But the protein itself, for all that, can remain bound to the RNA through another site as follows from our *in vitro* binding data and from the location of the binding site of rp eS1 in the cleft between SLI and SLIII resembling that on the 18S rRNA where rp eS1 is bound being in the 40S ribosomal subunit. Therefore, we conclude that when Sm proteins bind to the Sm site of the RNA that is currently being processed, rp eS1 proves to be associated with the RNA mainly through a site that is used by the protein when it interacts with the 18S rRNA and the N-terminal IDR of rp eS1 becomes free. Though the exact mechanism of the U11 pre-snRNA 3′-terminal processing is unknown, a significant increase in the level of U11 pre-snRNA and accordingly, a decrease in the level of U11 snRNA in rp eS1-depleted cells along with a reduction of the efficiency of splicing of the minor class introns strongly indicate an essential contribution of rp eS1 to the U11 snRNA biogenesis.

Although no rp eS1-bound U5 snRNA/U5 pre-snRNA was detected in nuclear and cytoplasmic cell fractions, considering our data on the in-cell rp eS1 cross-linking to RNA transcribed from the *RNU5A-1* gene, one can assume that rp eS1, when bound to U11 snRNP operating in splicing together with U5 snRNP, might simultaneously interact with U5 snRNA. It is generally accepted that at the initial steps of the minor class splicing, U11 snRNP recognizes the intron sequence adjacent to the 5′ splice site and forms, together with U12 snRNP, the minor pre-spliceosome (complex A) (35,36). The U5 snRNP joins the complex A as the tri-snRNP complex containing also U4atac and U6atac snRNPs to build the minor pre-catalytic spliceosome (complex B), which, in the result of a number of structural rearrangements, adopts the catalytically active configuration (complexes B*) similar to that in the major catalytic spliceosome (35,36). Although the composition of complex B corresponding to the minor spliceosome is unknown, analogous complex B for the major spliceosome comprises both U1 snRNA, functional analog of U11 snRNA and U5 snRNA (45,46). Hence, one can suppose that complex B for the minor spliceosome also contains both U11 and U5 snRNAs. This complex appears to be the only RNP, where U5 and U11 snRNP can occur alongside each other, because complex A does not yet contain U5 snRNA and complex B* does not already contain U11 snRNA. Importantly, U5 snRNA in the complex B interacts by its Loop I with the exon sequence neighboring the 5′ splice site of a minor intron, whereas U11 snRNA binds to the intron sequence adjacent to the 5′ splice site by the 5′-terminal region located near the H-helix (47,48). Thus, rp eS1 bound to U11 snRNA could reach U5 snRNA by its K-rich N-terminal IDR, which was identified as responsible for the protein cross-linking to 4-thiouridine-containing U11 snRNA *in vitro*, and could be a target for cross-linking of RNAs transcribed from the *RNU11* and *RNU5A-1* genes

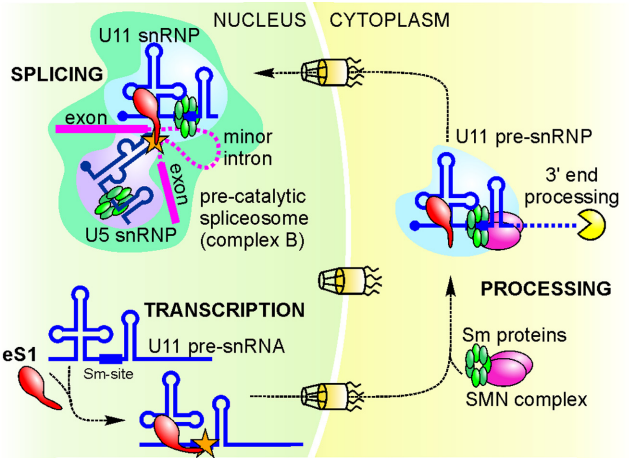

Figure 10. The scheme of the intended involvement of rp eS1 in cellular events related to U11 pre-snRNA processing and to minor class splicing. snRNAs are presented as the secondary structure skeletons, proteins are shown as colored balls, rp eS1 is depicted by red oval with the protruding N-terminal intrinsically disordered region.

in 4-thiouridine-treated cells. This interaction seems quite feasible because, as discussed above, the N-terminal IDR of rp eS1 should not be involved in the binding to U11 snRNA when its U-rich single-stranded sequence containing the portion of rp eS1 binding site is occupied by Sm proteins. Therefore, the above region of rp eS1 in mature U11 snRNP should be more flexible than in a complex where the protein is bound to U11 pre-snRNA. In the B complex, accordingly, the rp eS1 N-terminal IDR could interact with U11 snRNA through the SLI, SLIII and H-helix, and with U5 snRNA through Loop I, touching also Stems Ib and Ic located nearby it.

Thus, the data obtained in our study enable us to propose the following order of events in which rp eS1 is involved (Figure 10). Rp eS1 associates with the U11 pre-snRNA in the nucleus mainly through the interaction with SLI, SLIII, H-helix and the Sm site-containing U-rich single-stranded sequence that is bound to the protein N-terminal K-rich IDR, which causes conformational rearrangements in the U-rich region backbone (Figure 6). The resulting complex is then exported into the cytoplasm, where the SMN complex promotes the binding of Sm proteins to the pre-rearranged Sm site of U11 pre-snRNA, which is accompanied by the 3′-end processing of the RNA. After the processing completion, rp eS1-bound U11 snRNP is imported back into the nucleus, where rp eS1 is engaged in the minor class spliceosome assembly and interacts by its N-terminal IDR with U5 snRNAs at the 5′ splice site in the minor pre-catalytic spliceosome. The obtaining evidence for rp eS1 interactions with both U11 and U5 snRNAs in a pre-catalytic spliceosome is the next line of our investigations, in which a cross-linking approach utilizing a vast set of bifunctional reagents could be applied to nuclear cell fraction to identify the components bound to rp eS1.

Overall, the data obtained in this study, which is an initial step in exploring the functions of human ribosomal proteins beyond the ribosome by means of the PAR CLIP method, for the first time expose rp eS1 as an essential player in the

U11 pre-snRNA processing and indicate its involvement in events related to the minor splicing pathway, wherein the protein could interact with both U11 and U5 snRNAs. Our findings greatly expand the currently existing knowledge on extra-ribosomal functions of rp eS1, highlighting the N-terminal K-rich region of the protein as a key element responsible for its operation in the above processes.

ACCESSION NUMBERS

GenBank PRJNA337889, sample accession numbers SRP080974, SRS2126608–SRS2126613.

SUPPLEMENTARY DATA

Supplementary Data are available at NAR Online.

ACKNOWLEDGEMENTS

The authors are grateful to SB RAS Genomics Core Facility for the sequencing.

FUNDING

Russian Foundation for Basic Research [14-04-00740 and 17–04-00528 to A.A.M.]; SB RAS Complex scientific program [II.2П/VI.57–3 (0309–2015-0024) to G.G.K., in part]; State funded budget project [VI.57.1.2, 0309–2016-0001, in part]; Russian Ministry of Science and Education under 5–100 Excellence Programme, in part. Funding for open access charge: SB RAS Complex scientific program [II.2П/VI.57–3 (0309–2015-0024)].
Conflict of interest statement. None declared.

REFERENCES

1. Melnikov,S., Ben-Shem,A., Garreau de Loubresse,N., Jenner,L., Yusupova,G. and Yusupov,M. (2012) One core, two shells: bacterial and eukaryotic ribosomes. *Nat. Struct. Mol. Biol.*, **19**, 560–567.
2. Anger,A.M., Armache,J.P., Berninghausen,O., Habeck,M., Subklewe,M., Wilson,D.N. and Beckmann,R. (2013) Structures of the human and Drosophila 80S ribosome. *Nature*, **497**, 80–85.
3. Khatter,H., Myasnikov,A.G., Natchiar,S.K. and Klaholz,B.P. (2015) Structure of the human 80S ribosome. *Nature*, **520**, 640–645.
4. O'Donohue,M.F., Choesmel,V., Faubladier,M., Fichant,G. and Gleizes,P.E. (2010) Functional dichotomy of ribosomal proteins during the synthesis of mammalian 40S ribosomal subunits. *J. Cell Biol.*, **190**, 853–866.
5. Andersen,J.S., Lam,Y.W., Leung,A.K., Ong,S.E., Lyon,C.E., Lamond,A.I. and Mann,M. (2005) Nucleolar proteome dynamics. *Nature*, **433**, 77–83.
6. Malygin,A.A., Parakhnevitch,N.M., Ivanov,A.V., Eperon,I.C. and Karpova,G.G. (2007) Human ribosomal protein S13 regulates expression of its own gene at the splicing step by a feedback mechanism. *Nucleic Acids Res.*, **35**, 6414–6423.
7. Ivanov,A.V., Malygin,A.A. and Karpova,G.G. (2005) Human ribosomal protein S26 suppresses the splicing of its pre-mRNA. *Biochim. Biophys. Acta*, **1727**, 134–140.
8. Cuccurese,M., Russo,G., Russo,A. and Pietropaolo,C. (2005) Alternative splicing and nonsense-mediated mRNA decay regulate mammalian ribosomal gene expression. *Nucleic Acids Res.*, **33**, 5965–5977.
9. Graifer,D., Malygin,A., Zharkov,D.O. and Karpova,G. (2014) Eukaryotic ribosomal protein S3: a constituent of translational machinery and an extraribosomal player in various cellular processes. *Biochimie*, **99**, 8–18.
10. Mazumder,B., Sampath,P., Seshadri,V., Maitra,R.K., DiCorleto,P.E. and Fox,P.L. (2003) Regulated release of L13a from the 60S ribosomal subunit as a mechanism of transcript-specific translational control. *Cell*, **115**, 187–198.
11. Zhang,T., Chen,C., Breslin,M.B., Song,K. and Lan,M.S. (2014) Extra-nuclear activity of INSM1 transcription factor enhances insulin receptor signaling pathway and Nkx6.1 expression through RACK1 interaction. *Cell. Signal.*, **26**, 740–747.
12. Warner,J.R. and McIntosh,K.B. (2009) How common are extraribosomal functions of ribosomal proteins? *Mol. Cell*, **34**, 3–11.
13. des Georges,A., Dhote,V., Kuhn,L., Hellen,C.U., Pestova,T.V., Frank,J. and Hashem,Y. (2015) Structure of mammalian eIF3 in the context of the 43S preinitiation complex. *Nature*, **525**, 491–495.
14. Laletina,E., Graifer,D., Malygin,A., Ivanov,A., Shatsky,I. and Karpova,G. (2006) Proteins surrounding hairpin IIIe of the hepatitis C virus internal ribosome entry site on the human 40S ribosomal subunit. *Nucleic Acids Res.*, **34**, 2027–2036.
15. Babaylova,E., Graifer,D., Malygin,A., Stahl,J., Shatsky,I. and Karpova,G. (2009) Positioning of subdomain IIId and apical loop of domain II of the hepatitis C IRES on the human 40S ribosome. *Nucleic Acids Res.*, **37**, 1141–1151.
16. Malygin,A.A., Kossinova,O.A., Shatsky,I.N. and Karpova,G.G. (2013) HCV IRES interacts with the 18S rRNA to activate the 40S ribosome for subsequent steps of translation initiation. *Nucleic Acids Res.*, **41**, 8706–8714.
17. Yamamoto,H., Collier,M., Loerke,J., Ismer,J., Schmidt,A., Hilal,T., Sprink,T., Yamamoto,K., Mielke,T., Burger,J. *et al.* (2015) Molecular architecture of the ribosome-bound hepatitis C virus internal ribosomal entry site RNA. *EMBO J.*, **34**, 3042–3058.
18. Song,D., Sakamoto,S. and Taniguchi,T. (2002) Inhibition of poly(ADP-ribose) polymerase activity by Bcl-2 in association with the ribosomal protein S3a. *Biochemistry*, **41**, 929–934.
19. Cui,K., Coutts,M., Stahl,J. and Sytkowski,A.J. (2000) Novel interaction between the transcription factor CHOP (GADD153) and the ribosomal protein FTE/S3a modulates erythropoiesis. *J. Biol. Chem.*, **275**, 7591–7596.
20. Das,P., Basu,A., Biswas,A., Poddar,D., Andrews,J., Barik,S., Komar,A.A. and Mazumder,B. (2013) Insights into the mechanism of ribosomal incorporation of mammalian L13a protein during ribosome biogenesis. *Mol. Cell. Biol.*, **33**, 2829–2842.
21. Hafner,M., Landthaler,M., Burger,L., Khorshid,M., Hausser,J., Berninger,P., Rothballer,A., Ascano,M. Jr, Jungkamp,A.C., Munschauer,M. *et al.* (2010) Transcriptome-wide identification of RNA-binding protein and microRNA target sites by PAR-CLIP. *Cell*, **141**, 129–141.
22. Huang,C. and Yu,Y.T. (2013) Synthesis and labeling of RNA in vitro. *Curr. Protoc. Mol. Biol.*, **102**, 4.15.1–4.15.14.
23. Yanshina,D.D., Bulygin,K.N., Malygin,A.A. and Karpova,G.G. (2015) Hydroxylated histidine of human ribosomal protein uL2 is involved in maintaining the local structure of 28S rRNA in the ribosomal peptidyl transferase center. *FEBS J.*, **282**, 1554–1566.
24. Brummelkamp,T.R., Bernards,R. and Agami,R. (2002) A system for stable expression of short interfering RNAs in mammalian cells. *Science*, **296**, 550–553.
25. Alioto,T.S. (2007) U12DB: a database of orthologous U12-type spliceosomal introns. *Nucleic Acids Res.*, **35**(Suppl. 1), D110–D115.
26. DeLano,W.L. (2002) PyMol Molecular Graphics System User's Manual. DeLano Scientific, Palo Alto.
27. Pettersen,E.F., Goddard,T.D., Huang,C.C., Couch,G.S., Greenblatt,D.M., Meng,E.C. and Ferrin,T.E. (2004) UCSF Chimera—a visualization system for exploratory research and analysis. *J. Comput. Chem.*, **25**, 1605–1612.
28. Wang,L., Huang,C., Yang,M.Q. and Yang,J.Y. (2010) BindN+ for accurate prediction of DNA and RNA-binding residues from protein sequence features. *BMC Syst. Biol.*, **4**(Suppl. 1), S3.
29. Behrmann,E., Loerke,J., Budkevich,T.V., Yamamoto,K., Schmidt,A., Penczek,P.A., Vos,M.R., Burger,J., Mielke,T., Scheerer,P. *et al.* (2015) Structural snapshots of actively translating human ribosomes. *Cell*, **161**, 845–857.
30. Krol,A., Gallinaro,H., Lazar,E., Jacob,M. and Branland,C. (1981) The nuclear 5S RNAs from chicken, rat and man. U5 RNAs are encoded by multiple genes. *Nucleic Acids Res.*, **9** 769–787.

31. Montzka,K.A. and Steitz,J.A. (1988) Additional low-abundance human small nuclear ribonucleoproteins: U11, U12, etc. *Proc. Nat. Acad. Sci. U.S.A.*, **85**, 8885–8889.
32. Will,C.L. and Luhrmann,R. (2001) Spliceosomal UsnRNP biogenesis, structure and function. *Curr. Opin. Cell Biol.*, **13**, 290–301.
33. Patel,S.B. and Bellini,M. (2008) The assembly of a spliceosomal small nuclear ribonucleoprotein particle. *Nucleic Acids Res.*, **36**, 6482–6493.
34. Yong,J., Kasim,M., Bachorik,J.L., Wan,L. and Dreyfuss,G. (2010) Gemin5 delivers snRNA precursors to the SMN complex for snRNP biogenesis. *Mol. Cell*, **34**, 551–562.
35. Patel,A.A. and Steitz,J.A. (2003) Splicing double: insights from the second spliceosome. *Nat. Rev. Mol. Cell Biol.*, **4**, 960–970.
36. Turunen,J.J., Niemelä,E.H., Verma,B. and Frilander,M.J. (2013) The significant other: splicing by the minor spliceosome. *Wiley Interdiscip. Rev. RNA*, **4**, 61–76.
37. Jakel,S., Mingot,J.M., Schwarzmaier,P., Hartmann,E. and Gorlich,D. (2002) Importins fulfil a dual function as nuclear import receptors and cytoplasmic chaperones for exposed basic domains. *EMBO J.*, **21**, 377–386.
38. Gopanenko,A.V., Malygin,A.A. and Karpova,G.G. (2015) Exploring human 40S ribosomal proteins binding to the 18S rRNA fragment containing major 3′-terminal domain. *Biochim. Biophys. Acta*, **1854**, 101–109.
39. Moazed,D., Stern,S. and Noller,H.F. (1986) Rapid chemical probing of conformation in 16S ribosomal RNA and 30S ribosomal subunits using primer extension. *J. Mol. Biol.*, **187**, 399–416.
40. Latham,J.A. and Cech,T.R. (1989) Defining inside and outside of a catalytic RNA molecule. *Science*, **245**, 276–282.
41. Mortimer,S.A. and Weeks,K.M. (2007) A fast-acting reagent for accurate analysis of RNA secondary and tertiary structure by SHAPE chemistry. *J. Am. Chem. Soc.*, **129**, 4144–4145.
42. Pomeranz Krummel,D.A., Oubridge,C., Leung,A.K., Li,J. and Nagai,K. (2009) Crystal structure of human spliceosomal U1 snRNP at 5.5 A resolution. *Nature*, **458**, 475–480.
43. Will,C.L., Schneider,C., Hossbach,M., Urlaub,H., Rauhut,R., Elbashir,S., Tuschl,T. and Luhrmann,R. (2004) The human 18S U11/U12 snRNP contains a set of novel proteins not found in the U2-dependent spliceosome. *RNA*, **10**, 929–941.
44. Wahl,M.C., Will,C.L. and Lührmann,R. (2009) The spliceosome: design principles of a dynamic RNP machine. *Cell*, **136**, 701–718.
45. Will,C.L. and Lührmann,R. (2011) Spliceosome structure and function. *Cold Spring Harb. Perspect. Biol.*, **3**, a003707.
46. Matera,A.G. and Wang,Z. (2014) A day in the life of the spliceosome. *Nat. Rev. Mol. Cell Biol.* **15**, 108–121
47. Kolossova,I. and Padgett,R.A. (1997) U11 snRNA interacts in vivo with the 5′ splice site of U12-dependent (AU-AC) pre-mRNA introns. *RNA*, **3**, 227–233.
48. Yu,Y.T. and Steitz,J.A. (1997) Site-specific crosslinking of mammalian U11 and u6atac to the 5′ splice site of an AT-AC intron. *Proc. Nat. Acad. Sci. U.S.A.*, **94**, 6030–6035.